Separating phases of allopolyploid evolution with resynthesized and natural *Capsella bursa-pastoris*

Tianlin Duan[1,§], Adrien Sicard[2], Sylvain Glémin[1,3], Martin Lascoux[1]

[1] Department of Ecology and Genetics, Evolutionary Biology Centre and Science for Life Laboratory, Uppsala University, 75236 Uppsala, Sweden

[2] Department of Plant Biology, Swedish University of Agricultural Sciences, 75007 Uppsala, Sweden

[3] UMR CNRS 6553 ECOBIO, Campus Beaulieu, bât 14a, p.118, CS 74205, 35042 Rennes, France

[§]**Corresponding author:**

Tianlin Duan (tianlin.duan42@gmail.com)

Running title: From resynthesized to established allopolyploids

Keywords: Polyploidy; Selfing syndrome**;** Synapsis; Hybridization**;** Neopolyploid lines; Gene expression; *Capsella bursa-pastoris*

Author Contributions: All authors designed the study; TD and AS performed experiments; TD analyzed the data and drafted the manuscript. All authors edited it. All authors read and approved the final version of the manuscript.

Summary

Allopolyploidization is a frequent evolutionary transition in plants that combines whole-genome duplication (WGD) and interspecific hybridization. The genome of an allopolyploid species results from initial interactions between parental genomes and long-term evolution. Telling apart the contributions of these two phases is essential to understand the evolutionary trajectory of allopolyploid species. Here, we compared phenotypic and transcriptomic changes in natural and resynthesized *Capsella* allotetraploids with their diploid parental species. We focused on phenotypic traits associated with the selfing syndrome and on transcription-level phenomena such as expression level dominance (ELD), transgressive expression (TRE), and homoeolog expression bias (HEB).

We found that selfing syndrome, high pollen and seed quality in natural allotetraploids likely resulted from long-term evolution. Similarly, TRE and most down-regulated ELDs were only found in natural allopolyploids. Natural allotetraploids also had more ELDs toward the self-fertilizing parental species than resynthesized allotetraploids, mirroring the establishment of the selfing syndrome. However, short-term changes mattered, and 40% of ELDs in natural allotetraploids were already observed in resynthesized allotetraploids. Resynthesized allotetraploids showed striking HEB variation among chromosomes and individuals. Homoeologous synapsis was its primary source and may still be a source of genetic variation in natural allotetraploids.

In conclusion, both short- and long-term mechanisms contributed to transcriptomic and phenotypic changes in natural allotetraploids. However, the initial gene expression changes were largely reshaped during long-term evolution leading to further morphological changes.

225 words

Introduction

Allopolyploidization is the coupling of whole genome duplication and interspecific hybridization, resulting in organisms possessing two or more diverged genomes. This intriguing evolutionary transition is widespread in nature (Albertin & Marullo, 2012; Barker *et al.*, 2016), and is of agricultural importance (Behling *et al.*, 2019). Allopolyploidization is expected to have both short-term and long-term consequences: not only can the merging of divergent genomes itself be seen as a macromutation, but it also triggers subsequent genomic changes over distinct time scales.

Right after allopolyploidization or within a few generations, various genomic and transcriptomic changes can be caused by a series of mechanisms, including DNA methylation repatterning (Edger *et al.*, 2017; Li *et al.*, 2019), reactivation of transposable elements (TE, reviewed in Vicient & Casacuberta, 2017), chromosome rearrangements, including homoeologous exchanges (Parisod *et al.*, 2009; Szadkowski *et al.*, 2010; Lashermes *et al.*, 2014; Xiong *et al.*, 2021), and intergenomic interactions between regulatory elements (Shi *et al.*, 2012; Hu & Wendel, 2019). These multifaceted effects were initially proposed to be dramatic but are likely smoother and more subtle than initially thought. The fact remains that these short-term mechanisms add further complexity to the genetic variation gathered from parental lineages. Genetic changes can reinforce some initial epigenetic changes, leading to long-term heritable consequences in established allopolyploids. For instance, an epigenetically downregulated/silenced gene copy is more likely to degenerate than the other copy due to weaker purifying selection.

Apart from instant genomic changes, allopolyploidization also alters multiple genetic attributes, impacting the long-term evolution of allopolyploid genomes. First, as a minority cytotype, newly formed allopolyploid populations often experience a bottleneck (Levin, 1975; Novikova *et al.*, 2017; Griffiths *et al.*, 2019). This bottleneck reduces genetic variation within allopolyploid species and favors the fixation of neutral or slightly deleterious mutations (Novikova *et al.*, 2017). Second, with an extra genome, allotetraploid species could undergo a period of relaxed purifying selection (Lynch & Conery, 2000; Douglas *et al.*, 2015; Paape *et al.*, 2018). Relaxed selection also accelerates the accumulation of deleterious mutations on allopolyploid genomes. At the same time, it facilitates neofunctionalization by allowing functional mutations to accumulate in one paralog while maintaining the ancestral function through the second (Ohno, 1970). Third, allopolyploidization immediately distorts both the relative and absolute dosage of gene product, which further alters physiological balance and efficiency (Anneberg & Segraves, 2020; Yu *et al.*, 2021; Domínguez-Delgado *et al.*, 2021). In the long term, both relative and absolute dosages of gene expression of allopolyploid genomes are expected to be under selection (Bekaert *et al.*, 2011), and gradually adapt to a polyploid or hybrid state (Bomblies, 2020). Under the joint action of these forces, allopolyploid subgenomes are further coordinated and degenerated, and subgenomes are often biasedly fractionated (Schnable *et al.*, 2011; Tang *et al.*, 2012;

Renny-Byfield *et al.*, 2015; Wendel *et al.*, 2018).

Both short-term reactions and long-term evolution can generate novel evolutionary opportunities and potentially allow allopolyploid lineages to have advantages in adaptation to novel environments (Baniaga *et al.*, 2020). In established allopolyploids, phenomena caused by long-term evolutionary forces can be confounded by traces of short-term genomic changes. The relative contributions of short- and long-term mechanisms to genomic changes in allopolyploids can be assessed by comparing established natural allopolyploids with resynthesized allopolyploids (e.g., Wang *et al.*, 2006, 2016; Buggs *et al.*, 2011; Yoo *et al.*, 2013; Zhang *et al.*, 2016b).

Variation and novelties in gene expression caused by allopolyploidization are often assessed by homoeolog expression bias (HEB) and non-additive gene expression (Grover *et al.*, 2012; Yoo *et al.*, 2013; Zhang *et al.*, 2016a; Wu *et al.*, 2018; Shan *et al.*, 2020). Homoeolog expression bias measures the separate contributions of gene copies from different parental species (homoeologs) and non-additive gene expression measures the deviation of the total expression of both homoeologs from an intermediate value between parental species. Non-additive patterns of gene expressions are further classified as expression level dominance (ELD) and transgressive expression (TRE). ELD means that the total expression of both homoeologs is similar to the expression level of only one parental species (Grover *et al.*, 2012), but differs from the expression level of the other. TRE means that gene expression in allopolyploids is higher or lower than in both parental species. Variation of HEB and non-additive gene expression in allopolyploids can be triggered by several mechanisms in the early generations of the new allopolyploid; or alternatively, they may arise during long-term evolution due to either neutral or selective processes.

Capsella bursa-pastoris is a natural allotetraploid plant species which originated about 100,000 years ago (Douglas *et al.*, 2015). Two diploid species, *C. orientalis* and *C. grandiflora*, are extant relatives of the maternal and paternal progenitors (hereinafter referred to as parental species) of *C. bursa-pastoris*, respectively (Hurka *et al.*, 2012; Douglas *et al.*, 2015). *C. grandiflora* is self-incompatible (SI), but *C. orientalis* was already self-compatible (SC) before the formation of *C. bursa-pastoris* (Bachmann *et al.*, 2019). *C. bursa-pastoris* is also an SC species, with typical selfing-syndrome characteristics. In particular, it has smaller petals, fewer pollen grains, and shorter styles than the outcrossing *C. grandiflora* (Neuffer & Paetsch, 2013). Yet, it remains unclear whether the inconspicuous flower phenotypes of *C. bursa-pastoris* only reflect the dominance relationship of the parental alleles or if these traits have also evolved post-allopolyploidization.

Natural *C. bursa-pastoris* exhibits disomic inheritance (Hurka *et al.*, 1989; Roux & Pannell, 2015), although the strictness of disomic inheritance has not been tested. In general, the two subgenomes of *C. bursa-pastoris* are still well-retained and functional. There is no sign of large-scale gene loss or silencing, although purifying selection has

been weaker genome-wide (Douglas *et al.*, 2015), and the *C. orientalis*-derived subgenome (Cbp_co) has accumulated more putatively deleterious mutations than the *C. grandiflora*-derived subgenome (Cbp_cg), both before and after the formation of *C. bursa-pastoris* (Douglas *et al.*, 2015; Kryvokhyzha *et al.*, 2019a). The majority of genes were expressed from both homoeologs, and on average HEB was only slightly biased toward Cbp_cg homoeologs (Douglas *et al.*, 2015; Kryvokhyzha *et al.*, 2019a). Most genes are additively expressed in natural *C. bursa-pastoris*, but ELD and TRE have also been observed (Kryvokhyzha *et al.*, 2019a). Despite the moderate HEB and non-additive expression, gene expression in *C. bursa-pastoris* showed some striking tissue-specific features (Kryvokhyzha *et al.*, 2019a). In flowers, gene expression levels in *C. bursa-pastoris* resembled those in *C. orientalis*, while in leaves and roots, gene expression levels were more similar to those in *C. grandiflora.*

In contrast to the drastic genomic or transcriptomic changes observed in allopolyploid wheat (Zhang *et al.*, 2016a), *Brassica* (Szadkowski *et al.*, 2010; Lloyd *et al.*, 2018), and *Tragopogon* (Chester *et al.*, 2012), natural *C. bursa-pastoris* represents another paradigm where established allopolyploid species show only mild genomic changes and expression bias. This contrast raises questions. Was the genome of natural *C. bursa-pastoris* less affected by putative short-term mechanisms, or was it the result of 100,000 years' evolution, which filtered out or compensated for the initial drastic changes? What are the relative strengths of short-term mechanisms and long-term evolution in shaping genomic and phenotypic variation in allopolyploids?

Resynthesized allopolyploids are the closest approximation to the early stage of natural allopolyploids. They provide a reference point for separating the short-term effects of allopolyploidization from long-term evolutionary changes. The present study builds upon Duan *et al.* (2023), which showed that hybridization played a much larger role than whole genome doubling during the creation of resynthesized polyploids in the *Capsella* genus. Here, we compared transcriptomes and phenotypes of resynthesized *C. bursa-pastoris*-like allotetraploids with natural *C. bursa-pastoris* and its two diploid progenitors. We focused on teasing apart the contributions from short- and long-term processes to 1) phenotypes, 2) non-additive gene expression, and 3) homoeolog expression bias in *Capsella* allotetraploids.

Results

The selfing syndrome was observed in natural C. bursa-pastoris but not in resynthesized allotetraploids

The breakdown of self-incompatibility in allotetraploid *Capsella* can directly result from hybridizing with the self-fertilizing species (Bachmann *et al.*, 2021; Duan *et al.*, 2023). We explored to what extent the development of a selfing syndrome was instantly achieved after allopolyploidization or, instead, developed later on by comparing phenotypes of resynthesized allotetraploids (groups Sd and Sh), natural *C. bursa-*

pastoris (Cbp) and the diploid parental species, *C. grandiflora* (Cg2) and *C. orientalis* (Co2). The resynthesized allotetraploids were generated with individuals from one population of each diploid parental species (Fig. 1), and the Sd ("WGD-first") and Sh ("hybridization-first") groups only differed in the order of WGD and hybridization (Duan *et al.*, 2023). There were six "lines" in each of the five plant groups. For the Sd and Sh groups, each line represented an independent allopolyploidization event, while the six lines of natural Cbp were from six different populations (Fig. 1c and Table S1), representing three major genetic clusters of the wild *C. bursa-pastoris* (Kryvokhyzha *et al.*, 2016, 2019b). For diploid parental groups, a line referred to a full-sibling family resulting from self-fertilization (Co2) or one controlled cross (Cg2). Phenotypes of the five groups were measured in a growth chamber on about 36 individuals per plant group (6 individuals × 6 lines).

Resynthesized allotetraploids and the natural Cbp had distinct floral morphologies (Fig. 1a-g). Indeed, natural Cbp flowers had significantly shorter and narrower petals, sepals and pistils and shorter stamina than resynthesized allotetraploids (one-way ANOVA, $F_{4,162} > 76$ and $p < 0.001$ in all seven tests; Tukey's HSD test, $\alpha = 0.01$). Pollen and seed production was also affected. The number of pollen grains per flower decreased in natural Cbp (Fig. 1i). While the number of pollen grains in resynthesized allotetraploids was intermediate between the two parental species, the number of pollen grains of the Cbp group was now similar to that of the Co2 group (one-way ANOVA, $F_{4,137} = 164.6$, $p < 0.001$; Tukey's HSD test, $\alpha = 0.01$). On the other hand, the number of seeds per fruit in natural Cbp was much larger than in resynthesized allotetraploids. The resynthesized allotetraploids had a similar number of seeds in 10 fruits to that of the Cg2 group, whereas the number of seeds in 10 fruits in natural Cbp was even higher than that of the Co2 group (Fig. 1j; one-way ANOVA, $F_{4,146} = 152.5$, $p < 0.001$; Tukey's HSD test, $\alpha = 0.01$).

The architecture and phenology of the whole plant were affected too. The stem length of natural Cbp was shorter than in resynthesized allotetraploids, but was similar to the stem length of the Co2 group (Fig. 1h; one-way ANOVA, $F_{4,166} = 84.5$, $p < 0.001$; Tukey's HSD test, $\alpha = 0.01$). Finally, plants of the Cbp group flowered earlier than those of the Sd group, but at a similar time as those of the Sh group (Fig. 1k; one-way ANOVA with hc3 White's correction, $F_{4,165} = 49.2$, $p < 0.001$; Tukey's HSD test, $\alpha = 0.01$).

Pollen viability and seed quality improved in natural Capsella allotetraploids

Pollen viability and the proportion of normal seeds were compared between resynthesized and natural allotetraploids. For both traits, we observed a decrease in pollen viability in resynthesized allotetraploids followed by recovery in natural Cbp. Both Sd and Sh groups had lower proportions of viable pollen than the diploid parental species, but the proportion of viable pollen in natural Cbp was similar to that of the diploid parental species (Fig. 1l; GLM, quasi binomial, $F_{4,137} = 24.4$, $p < 0.001$; Tukey's HSD test, $\alpha = 0.01$). The resynthesized allotetraploids generated a higher proportion of

abnormal seeds than the three natural species (Fig. 1m; GLM, quasi binomial, $F_{4,146}$ = 59.2, $p < 0.001$; Tukey's HSD test, $\alpha = 0.01$). The average percentage of normal seeds was 69.6±4.3% in the Sd group and 77.5±2.2% in the Sh group. In contrast, the natural Cbp had almost no abnormal seeds, with a percentage of normal seeds of 99.6±0.8%.

A two-step evolution of the global expression pattern of natural allopolyploid Cbp

To compare the gene expression pattern of the five plant groups, RNA-sequencing was conducted for one individual per line and six lines per group, using young inflorescences (flowers) and leaves, respectively. Expression levels were determined for 21,937 genes in flower samples and 18,999 genes in leaf samples after excluding genes with CPM > 1 in less than two samples. The overall gene expression pattern was visualized with multi-dimensional scaling (MDS) analysis (Fig. 3a,b). For unphased gene expression, the resynthesized allotetraploids lay between the diploid parental species in both flowers and leaves. Natural Cbp samples were also intermediate between parental species in the first dimension but were far from the resynthesized allotetraploids in the other dimension, showing the effect of long-term evolution in Cbp and possibly also the divergence between extant diploid species and the real progenitors.

The expression levels of separate homoeologs in allotetraploids were determined with the diagnostic SNPs between the two diploid species. For the Sd, Sh, and Cbp groups, 52.8%, 53.7%, and 44.7% of the mapped reads could be assigned to one of the homoeologs, respectively. The expression pattern of each allotetraploid subgenome was more similar to the corresponding diploid progenitor (Fig. 3c,d). The pattern of expression of resynthesized allotetraploids was intermediate between those of diploid progenitors and natural Cbp.

Differential expression analysis was performed among the five plant groups, using the down-sampled unphased gene expression data. With a threshold of FC > 2 and FDR < 0.05, no significant differentially expressed genes (DEGs) were found between the two resynthesized allotetraploid groups, while 311 to 2888 DEGs were revealed in other group contrasts (Fig. S2,S3). There are two salient features. First, compared to either diploid progenitor, most DEGs in both resynthesized and natural allotetraploid groups were up-regulated (Fig. S3). The proportion of down-regulated DEGs increased, nevertheless, in natural allotetraploids. Second, both resynthesized allotetraploids, Sd and Sh, have much more DEG with Co2 than with Cg2. However, this is no longer the case in Cbp where the two comparisons yielded similar results.

Both short- and long-term mechanisms contributed to ELDs in natural Cbp, but TREs were mainly from long-term evolution

Non-additive gene expression shared by natural allotetraploids may be triggered right after allopolyploidization by short-term deterministic mechanisms, such as intergenomic interactions of regulatory elements. Alternatively, non-additive

expression may have been caused by mechanisms with stochastic effects or arose later during long-term evolution. We explored to what extent the non-additive expression shared by natural allotetraploids could reflect short-term deterministic mechanisms. By comparing gene expression levels in allotetraploids and diploid species, 21,647 genes in flowers and 18,758 genes in leaves were classified into one of the ten expression categories, using the results of DE analysis on unphased gene expression (FC > 2 and FDR < 0.05). We focused on complete ELDs and TREs: complete ELD is obtained when the gene expression level in an allopolyploid group is similar to that in one diploid group but not to the expression in the other diploid group, and TRE is detected when the gene expression level in an allopolyploid group is either higher or lower than in both diploid groups.

The percentage of genes showing complete ELD was altogether limited but doubled between resynthesized allotetraploid groups and natural allotetraploids (5.5% of genes in the former and 10.2% in the latter. Table S3 and Fig. 4a,b). ELD genes and their directions were highly shared between the two resynthesized allotetraploid groups (Figs 4c, S4) The majority of these shared ELDs were retained in natural allotetraploids (63.3% in flowers and 72.2% in leaves), suggesting that short-term deterministic mechanism contributed to ELD in natural Cbp. However, Cbp-specific ELDs were also abundant, comprising more than half of the ELDs found in the Cbp group (56.6% in flowers and 60.8% in leaves), thereby showing the effects of long-term evolution.

The direction of ELDs shifted between the resynthesized allotetraploids and natural Cbp (Table S3 and Fig. 4a,b). In resynthesized allotetraploids, most ELDs were up-regulated, and the number of ELDs toward *C. grandiflora* (Cg-ELD) was about twice of that toward *C. orientalis* (Co-ELD). Cbp still had more up-regulated ELDs than down-regulated ELDs, but the proportion of down-regulated ELDs increased. The proportion of Co-ELD had also increased in Cbp. In flowers, Cbp had more Co-ELD (1101) than Cg-ELD (938), and the number of Cg- and Co-ELDs were similar in leaves (Cg-ELD: 854, Co-ELD: 839).

Almost no TRE was found in resynthesized allotetraploids (less than five genes in either Sd or Sh group and in either tissue, Table S3 and Fig. 4a,b). In contrast, about 1.3% of genes in Cbp showed TRE in both flowers and leaves.

Segregation and recombination of homoeologous chromosomes were a major source of homoeolog expression bias (HEB) variation in resynthesized Capsella allotetraploids

Homoeolog expression bias (HEB) of genes in an allotetraploid individual was measured by the ratio of expression of the *C. grandiflora*-origin homoeolog (cg) to the total expression of both homoeologs (HEB = cg/(cg+co)). To obtain a reliable gene expression ratio, lowly expressed genes (CPM(cg+co) < 1 in any allotetraploid individual) were excluded from this analysis. Eventually, HEB was calculated for 18,255 genes in flowers, and 15,581 genes in leaves.

Overall, none of the three allotetraploid groups showed a strong average gene HEB. In flowers, the average gene HEB was 0.499±0.001, 0.531±0.001 and 0.475±0.001 for the Sd, Sh and Cbp groups, respectively. In leaves, the average gene HEB was 0.504±0.001, 0.532±0.001 and 0.477 for the Sd, Sh, and Cbp groups. When averaged among individuals, gene HEB of resynthesized allotetraploids had smaller gene-wise variation than that of the Cbp group (Levene's test, p-value < 0.001).

Among resynthesized allotetraploids, although the average HEB was not systematically biased toward Cg or Co, gene HEB showed great variation among chromosomes and individuals (Figs 5a,b,S5,S6). The distribution of HEB in some chromosomes had peaks around 0, 0.25, 0.75, or 1, but the shape of the distribution was almost identical between flower and leaf samples. When gene HEB was plotted along chromosomal positions, we found that the extra peaks in HEB distribution of resynthesized allotetraploids can be further explained by large genomic segments separated by a sudden change of average HEB (Figs 5c and S7-S10). Altogether, the pattern suggested that some chromosomes or chromosomal regions in resynthesized allotetraploids had an unbalanced number of cg- and co-homoeologs (not 2:2), which were likely caused by the segregation and recombination of homoeologous chromosomes. Both the segregation and recombination of homoeologous chromosomes are outcomes of homoeologous synapsis, which reflects polysomic or mixed inheritance in resynthesized allopolyploids. For short, we refer to both segregation and recombination of homoeologous chromosomes as homoeologous synapsis.

The effect of possessing an unbalanced number of homoeologs largely increased the variation of HEB in resynthesized allotetraploids. The breakpoint between segments with distinct average HEB and the copy number of cg-homoeolog on each segment were estimated with a five-state Hidden Markov Model (HMM), using gene HEB along chromosomes (Fig 5c, S13). Among the 96 chromosome quartets (two pairs of homologous chromosomes) from the 12 resynthesized allotetraploid individuals, only 39 chromosome quartets showed no sign of homoeologous synapsis, i.e., no breakpoint was identified and the estimated number of cg-homoeolog across the chromosome was two. On average 0.833±0.097 (mean±se) breakpoint was identified for each chromosome quartet, and 31.0% of genes were estimated to have different numbers of cg- and co-homoeologs. Finally, for resynthesized allotetraploids, the estimated copy number of homoeologs was able to explain 48.4% and 46.8% of the variance of HEB in flowers and leaves, respectively (GLM with quasi-binomial error distribution, $p < 0.001$ in both tissues).

In contrast to resynthesized allotetraploids, the distribution of HEB of natural Cbp was similar among individuals and chromosomes (Figs 5a,b, and S6), although the HEB distribution of some chromosomes of Cbp also showed weak bumps around 0, 0.25, 0.75 or 1 (Figs 5b, and S6). We could not confidently estimate the number of homoeologs or the breakpoint of segments for Cbp with only RNA-sequencing data, as

segments resulting from homoeologous exchanges could be shorter in natural Cbp, and the signals of copy number could be blurred by the variance of regulatory divergence. Nevertheless, the HMM segmentation algorithm also identified some candidate segments of which the average HEB strongly deviated from 0.5. Some candidate segments were only shared by individuals from the same population (Figs 6, S11, S12).

Most resynthesized allotetraploids had less homoeolog expression loss than natural Cbp, but with extreme outliers

Loss of homoeolog expression is a common phenomenon in allopolyploid species, which can be caused by homoeolog loss or silencing (Buggs *et al.*, 2009; Cox *et al.*, 2014; Lashermes *et al.*, 2016). Loss of homoeolog expression may quickly arise after allopolyploidy, or alternatively, reflect a gradual biased gene fractionation during diploidization. We compared the extent of loss of homoeolog expression between resynthesized and natural *Capsella* allotetraploids, and among allotetraploid individuals.

The loss of homoeolog expression was identified from genes with medium to high expression levels in all individuals of the corresponding diploid species (Fig. 7) to reduce noise from RNA-sequencing and phasing. On average, only 1.0 % of these genes showed homoeolog-specific expression loss in natural Cbp. Most resynthesized allotetraploids have a lower level of homoeolog-specific expression loss than natural Cbp, but three individuals (Sd-6-4, Sd-8-5, and Sh-5-5) showed an extremely high level of homoeolog expression loss. The striking homoeolog expression loss in these three resynthesized allotetraploids was most likely caused by segregation and recombination of homoeologous chromosomes, as the extreme HEBs in the three outliers were restricted to chromosome 3, where the entire chromosome or a large chunk of the chromosome has only expression from one homoeolog (Fig. 5b, S7-S10).

Expression level dominance is caused by different mechanisms in resynthesized and natural allotetraploid

As homoeologous synapsis seemed to be a major cause of HEB and homoeolog-specific expression loss in resynthesized allotetraploids, we assessed whether it could have also played a role in the evolution of ELD. To do so, we explored the mechanism of ELD in resynthesized allotetraploids by comparing the gene expression change of separate homoeologs relative to the corresponding gene in diploid groups (log2FC(cg/Cg2) and log2FC(co/Co2)) among non-additive gene expression categories (Fig. 8).

For ELDs in resynthesized allotetraploids, different non-exclusive short-term mechanisms would produce different patterns of average expression change of EL-dominant (homoeolog derived from the diploid progenitor to which the total expression of both homoeologs was similar) and EL-recessive homoeologs (the opposite homoeolog), among genes with significant ELD: i) If ELDs were mainly

caused by possessing more than two copies of the EL-dominant homoeolog (due to the segregation or recombination of homoeologous chromosomes), we would expect on average the expression of EL-dominant homoeolog to increase, and EL-recessive homoeolog to decrease, in both up- down-regulated ELDs. ii) If ELDs were mainly caused by mechanisms with random effects, such as TE transposition, on average, there should be no large difference between the expression changes of EL-dominant and EL-recessive homoeologs. Because the occurrence and regulatory effects of new TE transpositions do not depend on the original relative expression level of the two homoeologs, i.e., the highly and lowly expressed homoeologs are equally likely to be up- or down-regulated by new TE transpositions. iii) Predictions for new intergenomic interactions of regulatory elements can be complex, but under a simple scenario (Hu & Wendel, 2019), ELDs may be caused by divergent trans-acting factors. In allopolyploids, stronger trans-acting factors act on the cis-regulatory elements of the opposite homoeolog, causing a similar regulatory effect if transcription rate were not limited by the concentration of these trans-regulators. If this mechanism were the main cause of ELD, on average the EL-recessive homoeolog should have the larger expression change in all categories of ELDs, while the expression of EL-dominant homoeolog is not expected to change. In all other cases, we would not have direct inference on the exact mechanism of ELD, but at least the three mechanisms listed above could not be the predominant cause of ELD.

Concerning the ELD genes found in resynthesized allotetraploids, the change of homoeolog expression fits the third scenario. In all four categories of ELD, the EL-recessive homoeolog had a larger average expression change in the same direction as ELD, while the average expression change of EL-dominant homoeolog was closer to zero (Table S4, Fig. 8, S14).

ELDs specific to natural Cbp showed a different pattern. Although the EL-recessive homoeolog still had a larger expression change, the EL-dominant also showed non-zero average expression change toward the direction of ELD, especially in Cg-ELD genes. For genes with Cbp-specific TRE, both homoeologs had expression change in the same direction of TRE (Table S4, Fig. 8, S14).

Discussion

Distinguishing parental legacy from the effects of evolutionary forces is essential for interpreting the outcome of allopolyploidization. The short-term genomic interactions in allopolyploids reflect the divergence of parental genomes (Johnson, 2010). In this sense, short-term transcriptomic changes in new allopolyploids are also part of parental legacy but are not observable with only information from diploid parental species. In this study, we used resynthesized *Capsella* allotetraploids as an approximation of the early stage of the natural allotetraploid species to separate and compare the short- and long-term transcriptomic and phenotypic changes. The timing and pattern of the variation also provided hints for locating the exact mechanism.

The extant diploid species were not the exact parental populations of natural *C. bursa-pastori*s, and the sampled diploid individuals were genetically closer to the resynthesized allotetraploids than to natural *C. bursa-pastoris*, potentially leading to an overestimation of the contribution of long-term mechanisms. However, the divergence between *C. grandiflora* and *C. orientalis* was much more ancient than the formation of *C. bursa-pastoris* (Douglas *et al.*, 2015). Therefore, the molecular divergence between *C. grandiflora* and *C. orientalis* after the formation of *C. bursa-pastoris* is only a small fraction of the total divergence. Besides, the mating system of the real parental populations of *C. bursa-pastoris* was likely the same as today: A nonfunctional self-incompatibility haplotype that was fixed in *C. orientalis* was also found in *C. bursa-pastoris*, suggesting that *C.orientalis* has become self-compatible before the formation of *C. bursa-pastoris* (Bachmann *et al.*, 2019); On the other hand, restoring the great polymorphism of functional self-incompatibility haplotypes from a self-compatible ancestral population is very unlikely, therefore self-incompatibility should be the ancestral state in *Capsella* and there must have been outcrossing individuals in the ancestral population of the (*C. grandiflora* + *C. rubella*) linage. As so far there is no evidence for other ghost self-fertilizing population splitting from the ancient (*C. grandiflora* + *C. rubella*) linage before the formation of *C. bursa-pastoris*, the most parsimonious hypothesis is that Cbp_cg subgenome originated from outcrossing individuals, although we cannot exclude the alternative hypothesis that the progenitor of Cbp_cg is self-fertilizing. For all these reasons, the resynthesized *Capsella* allotetraploids may still provide a realistic approximation to the early stages of natural *C. bursa-pastoris.*

Another limitation of using resynthesized allotetraploids is that we could not completely exclude the effect of colchicine treatment, even though we used second-generation allotetraploids (Münzbergová, 2017). Colchicine treatment could affect pollen and seed quality and the rate of homoeologous synapsis in resynthesized allotetraploids. Spontaneous *Capsella* allotetraploids have been repeatedly found among diploid hybrids that were not treated with colchicine solution (Bachmann et al., 2021, and own unpublished results). For future studies, these spontaneous allotetraploids would be excellent materials for accurately estimating the rate of homoeologous synapsis in newly formed *Capsella* allotetraploids. Nevertheless, the reported influence of colchicine treatments on the second generation of synthetic polyploids was either trivial (Husband *et al.*, 2016) or not in the same direction as our results (Münzbergová, 2017). Hence, the observed pollen and seed quality reduction and rampant homoeologous synapsis were unlikely pure artifacts from colchicine treatment.

Resynthesized and natural Capsella allotetraploids had distinct phenotypes

The most noticeable morphological difference between resynthesized and natural *Capsella* allotetraploids was related to the selfing syndrome. If natural *C. bursa-*

pastoris indeed originated from the hybridization between *C. grandiflora*-like outcrossing plants and *C. orientalis*-like self-fertilizing plants, the selfing syndrome in *C. bursa-pastoris* does not reflect the instant dominance effect of the *C. orientalis* alleles, but evolved afterward. Compared to second-generation resynthesized allotetraploids, natural *C. bursa-pastoris* had smaller floral organs, more pollen per flower, and a shorter stem length (Fig. 1). In particular, trait values of petal size and stamen length of the resynthesized allotetraploids had almost no overlap with natural *C. bursa-pastoris* but were similar to the outcrossing progenitor *C. grandiflora*. The shorter stem length in natural *C. bursa-pastoris* may reflect a shorter lifespan, which is also a feature of self-fertilizing species (Duminil *et al.*, 2009; Lesaffre & Billiard, 2020). A remaining question is whether the genetic basis of the selfing syndrome in *C. bursa-pastoris* is the same as in *C. orientalis*. Did the pre-existing selfing syndrome-related alleles from *C. orientalis* facilitate the evolution of selfing syndrome in *C. bursa-pastoris*? Was the selfing syndrome of *C. bursa-pastoris* established by silencing/replacing the *C. grandiflora* alleles or new regulations on both *C. orientalis* and *C. grandiflora* homoeologs?

Although the selfing syndrome in natural *C. bursa-pastoris* was most likely an adaptation to the change in mating system, these morphological changes may be accelerated by the compensation or adaptation to a polyploid state (Hollister, 2015). WGD directly increases the size of various types of cells (Beaulieu *et al.*, 2008; Katagiri *et al.*, 2016; Snodgrass *et al.*, 2017; Wilson *et al.*, 2021) and disturbs the efficiency of multiple physiological processes (Drake *et al.*, 2013; Bomblies, 2020). Compared to newly resynthesized autopolyploids, natural autopolyploid plants often have smaller cell or organ sizes (Maherali *et al.*, 2009; Münzbergová, 2017; Landis *et al.*, 2020), possibly driven by the demand for optimizing physiological processes or resource allocation (Roddy *et al.*, 2020; Domínguez-Delgado *et al.*, 2021). In the case of allotetraploid *Capsella*, the selection of selfing-syndrome-related traits and the adaptation to a polyploid state (e.g., decreasing the size of cell or organ for physiological efficiency or better energy allocation) may work synergistically and can be difficult to separate.

Apart from the selfing-syndrome-related traits, newly resynthesized *Capsella* allotetraploids had lower proportions of viable pollen (Fig. 1l) and normal seeds (Fig. 1m). In contrast, pollen and seed quality in natural *C. bursa-pastoris* were much higher, as good as for the diploid species. The higher pollen and seed quality in natural *C. bursa-pastoris* was possibly achieved by improving meiotic behaviors. Meiotic stabilization is another important aspect of adaptation to an allopolyploid state (Blasio *et al.*, 2022). Newly resynthesized allopolyploids suffer more often than natural allopolyploids, from frequent and severe meiosis abnormalities, which are associated with lower pollen viability and fertility in resynthesized allopolyploids (Szadkowski *et al.*, 2010; Zhang *et al.*, 2013; Henry *et al.*, 2014). The molecular basis of improved meiotic synapsis in natural allopolyploids is not completely clear, but several loci that suppress homoeologous synapsis or recombination are essential for the process

(Jenczewski *et al.*, 2003; Nicolas *et al.*, 2009; Greer *et al.*, 2012; Martín *et al.*, 2017). The exact mechanism of meiotic stabilization in natural *C. bursa-pastoris* needs further investigation.

The emergence of non-additive gene expression in allotetraploids was a two-stage process

Non-additive gene expression in allotetraploid *Capsella* was altogether limited and neither a complete relict of short-term genomic interactions nor entirely due to gradual divergence. We found that about 40% of ELDs in natural *C. bursa-pastoris* could already be found in the second generation of resynthesized allotetraploids (relict ELDs). Most of these relict ELDs and their directions were shared by the two resynthesized allotetraploid groups (Figs 4c, S4), suggesting that most relict ELDs were repeatable alterations. On the other hand, about 60% of ELDs were specific to natural *C. bursa-pastoris* (Figs 4c, S4), revealing the contributions from long-term evolution.

The relict ELDs and Cbp-specific ELDs differed in several features. While the vast majority of relict ELDs were up-regulated (97% in flowers and 88% in leaves), Cbp-specific ELDs had a more balanced number of up- and down-regulated ELDs (61% and 54% were up-regulated in flowers and leaves, respectively), suggesting the short and long-term ELDs had different molecular basis. In diploid or polyploid interspecific hybrids, overexpression is often more common than underexpression. The trend has been observed in a wide range of organisms, including *Brassica* (Wu *et al.*, 2018; Li *et al.*, 2020; Wei *et al.*, 2021), cotton (Yoo *et al.*, 2013), *Raphanobrassica* (Ye *et al.*, 2016), brown algae (Sousa *et al.*, 2019) and copepod (Barreto *et al.*, 2015). Results in *Capsella* further showed that short-term mechanisms mainly caused the excess of up-regulated ELDs. Among the short-term mechanisms, intergenomic interaction of regulatory elements is the most likely candidate for generating the excess of up-regulated ELDs, considering that these up-regulated ELDs were highly shared between the two resynthesized allotetraploid groups, and between resynthesized and natural allotetraploids. A global DNA methylation change may also contribute to the excess of up-regulation in resynthesized allotetraploids, if methylation levels were systematically lower in *Capsella* allotetraploids, as observed in *Mimulus* (Edger *et al.*, 2017). However, methylation change alone fails to explain why the majority of these up-regulated ELDs in resynthesized allotetraploids were retained in natural allotetraploids, especially in leaves (Fig. 4c, S4).

Besides, the relict ELDs contained more Cg-ELDs than Co-ELD, but Cbp-specific ELDs had more Co-ELDs, especially in flowers (Fig. 4c, S4). The increase of Co-ELDs in natural *C. bursa-pastoris* mirrored the morphological difference: The floral organ size of resynthesized allotetraploids was similar to that of *C. grandiflora*, whereas natural *C. bursa-pastoris* was more similar to *C. orientalis* (Fig. 1a-g). However, it is worth noting that the reversed trend of ELDs may not be the fundamental genetic basis of selfing syndrome, but reflect the different composition of tissue/cells in RNA

samples. Both morphological changes and the direction of ELDs could result from upstream regulatory changes.

In addition, although unbalanced homoeolog content (not 2:2) caused by homoeologous synapsis was common in our resynthesized allotetraploids, they were still not the main cause of ELD in resynthesized allotetraploids. If ELDs were mainly caused by possessing more than two copies of the EL-dominant homoeolog, we would expect the relative expression from EL-dominant homoeolog to increase and the EL-recessive homoeolog to decrease in genes with significant ELDs. In contrast to this expectation, we found that, on average, the expression of EL-dominant homoeologs (relative to the transcriptome of the subgenome) was similar to that in diploid parental species, while the expression of EL-recessive homoeologs changed toward the EL-dominant homoeolog (Fig. 8). This suggests that ELD is mainly achieved by altering the expression of EL-recessive homoeologs. This result is consistent with studies in a wide range of allopolyploid organisms (Yoo *et al.*, 2013; Cox *et al.*, 2014; Combes *et al.*, 2015; Sousa *et al.*, 2019), though not in resynthesized *Brasssica napus* (Wu *et al.*, 2018). This conservative pattern can be explained by intergenomic interaction between divergent regulatory elements (Hu & Wendel, 2019), but direct evidence is still lacking.

As for transgressive gene expression, we found almost no TRE genes in resynthesized allotetraploids, but a mere 1.3% TRE genes in natural *C. bursa-pastoris*, with a threshold of FC > 2 (Table S3). In agreement with several previous observations (Flagel & Wendel, 2010; Yoo *et al.*, 2013; Zhang *et al.*, 2016b), the results in *Capsella* suggest that transcriptional novelties in allopolyploids were not an instant outcome of allopolyploidization but mainly arose during long-term evolution and remained altogether rather limited.

Homoeologous synapsis was common in resynthesized Capsella allotetraploids, and may still be a source of variation in natural Cbp

Disomic inheritance in allopolyploid species is not established all at once (Henry *et al.*, 2014), and strict disomic inheritance may have never been achieved in some allopolyploid species. In contrast to the disomic inheritance and the low level of homoeolog expression loss in natural *C. bursa-pastoris*, we found abundant traces of homoeologous segregation or recombination in all twelve lines of resynthesized *Capsella* allotetraploids, after only one meiosis. The observation is in line with many recent studies in which abundant homoeologous exchanges were found in allopolyploids (Lloyd *et al.*, 2018; Pelé *et al.*, 2018). The contrast between resynthesized and natural allotetraploids suggested that preferential synapsis was rapidly improved in natural *C. bursa-pastoris*, and/or a balanced number of homoeologs was strongly preferred by selection, otherwise, we would expect a much higher proportion of homoeolog replacement (having four copies of the same homoeolog) after 100,000-year recurrent self-fertilization with tetrasomic/heterosomic inheritance.

Homoeologous synapsis was the major mechanism for HEB variation and homoeolog expression loss in resynthesized *Capsella* allopolyploids (Fig. 5,7). Several models have been proposed to explain HEB and biased genome fractionation in allopolyploids, including different TE contents (Woodhouse *et al.*, 2014; Cheng *et al.*, 2016; Wendel *et al.*, 2018), the epigenetic difference of subgenomes (Li *et al.*, 2014), different strength of regulatory elements, as a result of enhancer runaway (Fyon *et al.*, 2015; Bottani *et al.*, 2018). It was also suggested that the initial HEB may be reinforced in long-term evolution, as the homoeolog with a lower initial expression level is subject to weaker purifying selection, and has a larger chance of degeneration (Woodhouse *et al.*, 2014). However, in resynthesized *Capsella* allotetraploids, homoeologous synapsis played an important role in generating HEB variation, possibly overshadowing the influence of other mechanisms in generating HEB variation. This result does not conflict with the observed association between TE content in parental species and genome dominance (Woodhouse *et al.*, 2014). While TE contents may have only a minor effect in directly generating HEB variation, they could still be informative in predicting HEB in established allopolyploids, as the presence of TEs in the flanking regions may affect the fitness effect of HEB variation (Hollister & Gaut, 2009). In other words, TEs may not function as a strong mutagenic mechanism of HEB variation, but affect the selection on HEB variation, as a form of genetic load.

For established natural allotetraploids, occasional homoeologous synapsis may still be an important source of genetic variation, even long after the allopolyploidization event. Although an earlier allozymic study (Hurka *et al.*, 1989) and an approximate Bayesian computation (ABC) with high throughput sequencing data (Roux & Pannell, 2015) suggest that natural *C. bursa-pastoris* exhibits disomic inheritance, neither analysis could reject homoeologous synapsis at a lower rate. A very small proportion of homoeologous synapsis may be negligible for inferring the dominant mode of inheritance, but in terms of causing homoeologous gene loss and creating genetic variation, homoeologous synapsis can still be more influential than point mutations. Due to the inevitable technical variation of RNA-seq and expression variation across genes, we were unable to confidently resolve smaller blocks of unbalanced homoeolog content. Despite the small sample size and the low resolution of RNA-seq data, we noticed that some small genomic blocks with homoeolog replacement were shared by the individuals of the same population but varied among populations of natural *C. bursa-pastoris* (Figs 6, S11,S12), suggesting that homoeologous synapsis still contribute to expressional variation in natural *C. bursa-pastoris*. Apart from homoeolog synapsis in a single-origin allopolyploid species, unbalanced content of homoeologs could also arise from secondary introgression from diploid parental species. Detailed demographic modelling would be needed for distinguishing the two scenarios.

Conclusion

In conclusion, together with Duan *et al.* (2023), the present study shows that both short-

and long-term mechanisms contributed to transcriptomic and phenotypic changes in natural allotetraploids. However, the initial gene expression changes were largely reshaped during long-term evolution leading to more pronounced morphological changes. Resource limitations and/or adaptation to self-fertilization also, drive flowers' evolution after polyploidization.

Material and Methods

Plant material

The present study used five *Capsella* plant groups (Fig. 1 and Table S1), including diploid *C. orientalis* (Co2), diploid *C. grandiflora* (Cg2), two types of resynthesized allotetraploids (Sd and Sh), and natural allotetraploids, *C. bursa-pastoris* (Cbp). RNA-sequencing data and most phenotypic data (except floral morphologic traits) of Co2, Cg2, Sd, and Sh groups were from Duan *et al.* (2023). The Sd and Sh allotetraploids only differed in the order of hybridization and whole genome duplication. Allotetraploids of the Sd group were generated by crossing synthetic autotetraploid *C. orientalis* with autotetraploid *C. grandiflora*, whereas the Sh group was generated by inducing WGD in the first generation of diploid hybrids of *C. orientalis* × *C. grandiflora*. In all interspecific crosses, *C. orientalis* served as maternal plants, mimicking the formation of the natural allotetraploid species, *C. bursa-pastoris* (Hurka *et al.*, 2012). All *C. orientalis* plants used in the experiment are descendants of one wild *C. orientalis* individual, and all the *C. grandiflora* plants are descendants of three individuals from one *C. grandiflora* population (Fig. 1c and Table S1).

To compare the resynthesized allotetraploids with natural allotetraploids, natural *C. bursa-pastoris* was added to the present study. Seeds of wild *C. bursa-pastoris* plants were grown in a growth chamber for one generation. Then the second generation of *C. bursa-pastoris* plants was grown in the same experiment together with the other four plant groups used in Duan *et al.* (2023). All five groups were grown in a growth chamber under long-day conditions (16-h light at 22°C and 8-h dark at 20°C, light intensity=137 uE·m-2·s-1).

Each of the five groups was represented by six “lines”, and each line had six individuals, which were full siblings from either self-fertilization (Co2, Cbp, Sh, and Sd groups) or brother-sister mating (Cg2 group). The six lines of *C. bursa-pastoris* were from six populations (Fig. 1c and Table S1), representing three major genetic clusters of the wild *C. bursa-pastoris* (Kryvokhyzha *et al.*, 2019b). Each line originated from an independent allopolyploidization event for Sh and Sd groups. For Co2 and Cg2 groups, “line” only referred to the offspring of one parental plant (Co2) or a pair of parental plants (Cg2) in the previous generation.

Phenotyping

Floral morphological traits were measured for all five groups on 167 plants 7-14 days after the first flower opened. Two fully opened young flowers were dissected for each plant, and the floral organs were scanned with a photo scanner (Epson Perfection V370) at 3200 dpi. Seven floral morphological traits were measured on the digital images with Fiji, an open-source platform for biological-image analysis (Schindelin *et al.*, 2012), including sepal width, sepal length, petal width, petal length, pistil width, pistil length, and stamen length. For each plant, two flowers were examined. Three sepals, petals and stamina, and one pistil were measured for each flower.

For the Cbp group, stem length, flowering time, pollen count, pollen viability, and proportion of normal seeds were measured in the same way as the other four groups in Duan *et al.* (2023). In the case of Cg2 and Cg4, seeds were obtained through controlled pollination (Duan *et al.*, 2023). The length of the longest stem (stem length) was measured on dry plants. The number of days from germination start to the opening of the first flower was recorded as flowering time. The number of pollen grains per flower (pollen counts) was calculated by counting 1/60 (Co2, Sd, Sh, and Cbp groups) or 1/120 (Cg2 group) of the total pollen grains of a flower using a hemocytometer. Pollen viability was measured with an aceto-carmine staining method (Duan *et al.*, 2023), by examining at least 300 pollen grains per flower. Pollen counts and pollen viability were measured on two flowers of each individual. Seeds from the 11th to 20th fruits were counted and were used to measure the proportion of normal seeds. The first ten fruits were used when not all of these flowers set fruits. Individuals with less than ten fruits were excluded from the analysis. Seeds that were flat or dark and small were considered abnormal.

RNA-sequencing

RNA-sequencing was conducted for the five plant groups (Co2, Cg2, Sd, Sh, and Cbp). For each line, leaf and young inflorescence (flower) samples from one randomly chosen individual were sequenced, resulting in 60 RNA-sequencing samples (5 groups × 6 lines × 2 tissues). RNA-sequencing data of the Co2, Cg2, Sd, and Sh groups were from Duan *et al.* (2023). Data from the Cbp group was added to the present study, but the Cbp samples were collected and sequenced simultaneously with the other four plant groups in 2019. The 8th and 9th leaves were harvested at the emergence of the 11th leaf, and 2-4 inflorescences with only unopened flower buds were collected 7-14 days after the first flower opened. The collected tissue was frozen in liquid nitrogen and stored at -80 °C.

Total RNA was extracted from leaf and flower samples with a cetyl-trimethyl-ammonium-bromide (CTAB) based method (Duan *et al.*, 2023). DNA contamination was further removed by the RNase-Free DNase Set (QIAGEN). RNA libraries were prepared with Illumina TruSeq Stranded mRNA (poly-A selection) kits and sequenced with pair-end reads of 150 bp on three NovaSeq 6000 S4 lanes, by the SNP&SEQ

Technology Platform in Uppsala. One sequencing library was generated for each diploid sample, and two libraries were generated for each allotetraploid sample.

Gene and homoeolog expression

Raw RNA-seq reads were mapped to the reference genome of *Capsella rubella* (Slotte *et al.*, 2013) using Stampy v.1.0.32 (Lunter & Goodson, 2011). The expected divergence between reference and query sequences was set to 0.02, 0.04, and 0.025 for *C. grandiflora*, *C. orientalis,* and allotetraploids, respectively. Mapping quality was inspected by Qualimap v. 2.2.1 (Okonechnikov *et al.*, 2016). The number of reads mapped to each gene was counted by HTSeq v.0.12.4 (Anders *et al.*, 2015), using the mode "union" (hereinafter referred to as "unphased gene expression"). The average number of mapped reads was 38.4±2.4 and 70.0±3.5 for the diploid and tetraploid samples, respectively (Table S2). For all analyses on unphased gene expression, the mapped reads were downsampled with a custom Python script (Duan *et al.*, 2023), so that all five groups had a similar average number of mapped reads.

The expression level of separate homoeologs in allotetraploids was determined by the program HyLiTE v.2.0.2 (Duchemin *et al.*, 2015). Alignment results from the software Stampy v.1.0.32 (Lunter & Goodson, 2011) of all five groups and the *C. rubella* reference genome (Slotte *et al.*, 2013) were used as the input for HyliTE. HyLiTE performed SNP calling, classified RNA-seq reads of allotetraploids to parental types according to the identified diagnostic variation between the two diploid parental species and generated a table of homoeolog read counts for allotetraploid individuals (hereinafter referred to as "phased gene expression").

After partitioning the homoeolog expression, the average library size of allotetraploid subgenomes was similar to the library size of diploid groups (Fig. S1; one-way ANOVA, $F_{4,91}$=1.28, p = 0.29). To reduce bias between phased and unphased expression datasets, when the homoeolog expression of allotetraploids was compared with gene expression in diploid parental species, the expression level of each gene in diploid individuals was rescaled by the proportion of reads that can be phased for the same gene in allotetraploid individuals.

The overall gene expression pattern of five plant groups in each tissue was visualized by MDS analysis, using the R package edgeR (version 3.28.1; Robinson et al., 2010) in the R software environment version 3.6.3 (R Core Team, 2020). For both phased and unphased gene expression data, genes with count-per-million (CPM) over one in at least two samples were used for the MDS analysis, and expression levels were normalized with the trimmed mean of M-values (TMM) method.

Differential expression (DE) analysis

DE analysis was conducted on both unphased and phased gene expression data with the

R package edgeR (version 3.28.1; Robinson et al., 2010), using TMM normalized gene expression levels. A negative binomial generalized linear model (GLM) was fitted to each dataset. Pairwise group contrasts were then made for each GLM model, and gene-wise quasi-likelihood F-tests were conducted to detect expression changes in each contrast. For unphased data, pairwise contrasts were made among the original five groups (Co2, Cg2, Sd, Sh, and Cbp). For phased data, allopolyploid subgenomes were treated as separate groups (Sd_co, Sd_cg, Sh_co, Sh_cg, Cbp_co, and Cbp_cg) and were compared with the two diploid groups (Co2, Cg2). Genes with an expression fold-change (FC) larger than two and a false discovery rate (FDR) less than 0.05 were considered significant differentially expressed genes (DEGs).

Expression level dominance and transgressive expression

To measure the extent of non-additive expression in allotetraploids, genes were classified into ten expression categories (Table 1), by comparing the total expression of both homoeologs in an allotetraploid group to the gene expression level in a diploid group. The ten categories were modified from the classification by Zhang et al. (2016). Results of DE analysis on unphased gene expression (FC > 2 and FDR < 0.05) were used for the classification.

Homoeolog expression bias

Homoeolog expression bias of gene *i* in allotetraploid individual *j* was measured by the proportion of cg-homoeolog expression (cg_{ij}) in the total expression of both homoeologs (HEB = $cg_{ij}/(cg_{ij}+co_{ij})$). The distribution of HEB was then viewed by individuals, chromosomes or along genomic coordinates. Signs of the segregation or recombination of homoeologous chromosomes were revealed in resynthesized allopolyploids by HEB distribution along genomic coordinates.

The copy number of cg- and co-homoeologs of each gene and the breakpoints between chromosomal segments resulting from homoeologous recombination were estimated with a five-state Hidden Markov Model (HMM) of gene HEB, using a modified version of the R package HMMcopy version 1.40.0 (Lai *et al.*, 2022). The five states corresponded to (0, 1, 2, 3, 4) gene copies from Cg and (4, 3, 2, 1, 0) copies from Co, respectively. The expected optimal values of median HEB (*m*) were set to 0.01, 0.25, 0.5, 0.75 and 0.99 for the five states. The length of segments was controlled by arguments *e* and *strength*. *e* is the initial value of the transition probability that the state (copy number of cg homoeolog) does not change between two adjacent genes, and *strength* is the strength of this initial *e*. Smaller values of *strength* increase the flexibility of transition probability, and an extremely large value leads to almost fixed transition probabilities. For natural *C. bursa-pastoris*, *e* and *strength* were set to (1 − 1e-7) and 1e+7, respectively. For resynthesized allotetraploids, *e* was increased to (1 − 1e-10), and *strength* was increased to 1e+12, as homoeologous exchanges were expected to be rare for resynthesized allotetraploids which had only experienced one round of meiosis.

The effect of homoeologous segregation and recombination on HEB in resynthesized allotetraploids was analyzed by a generalized linear model with quasi-binomial error distribution and logit link function. Gene HEB was reshaped as binomial data (read counts from cg homeolog and total counts from both homoeologs). The copy number of cg homoeologs (0, 1, 2, 3, and 4) estimated by HMM segmentation was used as the explanatory variable. The variance of HEB explained by the estimated copy number of cg homoeolog was assessed by the coefficient of determination (R^2), calculated with "rsq" R package version 2.5 (Zhang, 2022).

The relationship between non-additive gene expression and homoeolog expression was explored by comparing the estimated expression fold change of each homoeolog among additive and different non-additive expression categories. The expression fold change of homoeologs was measured by homoeolog expression of gene *i* in allotetraploid group *k* divided by expression of gene *i* in the corresponding diploid group, i.e., $\log2FC(cg_{ik}/Cg2_i)$ or $\log2FC(co_{ik}/Co2_i)$, using the estimated FC from DE analysis on phased data. The difference of expression fold change between EL-dominant and EL-recessive homoeologs was tested by Welch's two-sample t-tests.

Loss of homoeolog expression

The most extreme HEB occurs when one homoeolog is silenced or lost in allotetraploids. To explore the timing and mechanism of the loss of homoeolog expression in *Capsella*, the number of genes with homoeolog expression loss was counted for each resynthesized or natural allotetraploid. Lowly or occasionally expressed genes were excluded from the analysis to reduce noise from sequencing and phasing. Specifically, if one homoeologous gene had obvious expression (CPM > 5) in all six individuals of the corresponding diploid species, but had almost no expression in one allotetraploid individual (CPM < 0.5), the case was considered a loss of homoeologous expression.

Acknowledgements

The study was supported by grant 2019-00806 from the Swedish Research Council to ML and Nilsson-Ehle research grant from the Royal Physiographic Society in Lund to TD. ML also acknowledges support from the Erik Philip-Sörensen Foundation. TD was supported by the Sven and Lilly Lawski Foundation. Computation and data handling were provided by the Swedish National Infrastructure for Computing (SNIC) at Uppmax, partially funded by the Swedish Research Council through grant agreement no. 2018-05973. We thank Barbara Mable for her critical comments on the manuscript. Finally, we thank Elsa Sundkvist and Mattias Vass for their help with seed collecting and counting.

Data availability

The RNA-sequencing data of natural *C. bursa-pastoris* generated by this article are available in NCBI Sequence Read Archive (SRA), and can be accessed with BioProject number PRJNA848625. BioSample accessions are listed in Table S2.

References

Albertin W, Marullo P. **2012**. Polyploidy in fungi: evolution after whole-genome duplication. *Proceedings of the Royal Society B: Biological Sciences* **279**: 2497–2509.

Anders S, Pyl PT, Huber W. **2015**. HTSeq-A Python framework to work with high-throughput sequencing data. *Bioinformatics* **31**: 166–169.

Anneberg TJ, Segraves KA. **2020**. Nutrient enrichment and neopolyploidy interact to increase lifetime fitness of *Arabidopsis thaliana*. *Plant and Soil* **456**: 439–453.

Bachmann JA, Tedder A, Fracassetti M, Steige KA, Lafon-Placette C, Köhler C, Slotte T. **2021**. On the origin of the widespread self-compatible allotetraploid *Capsella bursa-pastoris* (Brassicaceae). *Heredity* **127**: 124–134.

Bachmann JA, Tedder A, Laenen B, Fracassetti M, Désamoré A, Lafon-Placette C, Steige KA, Callot C, Marande W, Neuffer B, *et al.* 2019. Genetic basis and timing of a major mating system shift in Capsella. *New Phytologist* **224**: 505–517.

Baniaga AE, Marx HE, Arrigo N, Barker MS. **2020**. Polyploid plants have faster rates of multivariate niche differentiation than their diploid relatives. *Ecology Letters* **23**: 68–78.

Barker MS, Arrigo N, Baniaga AE, Li Z, Levin DA. **2016**. On the relative abundance of autopolyploids and allopolyploids. *New Phytologist* **210**: 391–398.

Barreto FS, Pereira RJ, Burton RS. **2015**. Hybrid Dysfunction and Physiological Compensation in Gene Expression. *Molecular Biology and Evolution* **32**: 613–622.

Beaulieu JM, Leitch IJ, Patel S, Pendharkar A, Knight CA. **2008**. Genome size is a strong predictor of cell size and stomatal density in angiosperms. *New Phytologist* **179**: 975–986.

Behling AH, Shepherd LD, Cox MP. **2019**. The importance and prevalence of allopolyploidy in Aotearoa New Zealand. *https://doi.org/10.1080/03036758.2019.1676797* **50**: 189–210.

Bekaert M, Edger PP, Chris Pires J, Conant GC. **2011**. Two-Phase Resolution of Polyploidy in the *Arabidopsis* Metabolic Network Gives Rise to Relative and Absolute Dosage Constraints. *The Plant Cell* **23**: 1719–1728.

Blasio F, Prieto P, Pradillo M, Naranjo T. **2022**. Genomic and Meiotic Changes Accompanying Polyploidization. *Plants* **11**.

Bomblies K. **2020**. When everything changes at once: finding a new normal after genome duplication. *Proceedings of the Royal Society B* **287**: 20202154.

Bottani S, Zabet NR, Wendel JF, Veitia RA. **2018**. Gene Expression Dominance in Allopolyploids: Hypotheses and Models. **23**: 393–402.

Buggs RJA, Doust AN, Tate JA, Koh J, Soltis K, Feltus FA, Paterson AH, Soltis PS, Soltis DE. **2009**. Gene loss and silencing in *Tragopogon miscellus* (Asteraceae): comparison of natural and synthetic allotetraploids. *Heredity 2009 103:1* **103**: 73–81.

Buggs RJA, Zhang L, Miles N, Tate JA, Gao L, Wei W, Schnable PS, Barbazuk WB, Soltis PS, Soltis DE. **2011**. Transcriptomic shock generates evolutionary novelty in a newly formed, natural allopolyploid plant. *Current Biology* **21**: 551–556.

Cheng F, Sun C, Wu J, Schnable J, Woodhouse MR, Liang J, Cai C, Freeling M, Wang X. **2016**. Epigenetic regulation of subgenome dominance following whole genome triplication in *Brassica rapa*. *New Phytologist* **211**: 288–299.

Chester M, Gallagher JP, Symonds VV, Da Silva AVC, Mavrodiev E V., Leitch AR, Soltis PS, Soltis DE. **2012**. Extensive chromosomal variation in a recently formed natural allopolyploid species, *Tragopogon miscellus* (Asteraceae). *Proceedings of the National Academy of Sciences of the United States of America* **109**: 1176–1181.

Combes MC, Hueber Y, Dereeper A, Rialle S, Herrera JC, Lashermes P. **2015**. Regulatory Divergence between Parental Alleles Determines Gene Expression Patterns in Hybrids. *Genome Biology and Evolution* **7**: 1110–1121.

Cox MP, Dong T, Shen GG, Dalvi Y, Scott DB, Ganley ARD. **2014**. An Interspecific Fungal Hybrid Reveals Cross-Kingdom Rules for Allopolyploid Gene Expression Patterns. *PLoS Genetics* **10**: 1004180.

Domínguez-Delgado JJ, López-Jurado J, Mateos-Naranjo E, Balao F. **2021**. Phenotypic diploidization in plant functional traits uncovered by synthetic neopolyploids in *Dianthus broteri*. *Journal of Experimental Botany* **72**: 5522–5533.

Douglas GM, Gos G, Steige KA, Salcedo A, Holm K, Josephs EB, Arunkumar R, Ågren JA, Hazzouri KM, Wang W, *et al.* 2015. Hybrid origins and the earliest stages of diploidization in the highly successful recent polyploid *Capsella bursa-pastoris*. *Proceedings of the National Academy of Sciences of the United States of America* **112**: 2806–2811.

Drake PL, Froend RH, Franks PJ. **2013**. Smaller, faster stomata: scaling of stomatal size, rate of response, and stomatal conductance. *Journal of Experimental Botany* **64**: 495–505.

Duan T, Sicard A, Glémin S, Lascoux M. **2023**. Expression pattern of resynthesized allotetraploid *Capsella* is determined by hybridization, not whole-genome duplication. *New Phytologist* **237**: 339–353.

Duchemin W, Dupont PY, Campbell MA, Ganley ARD, Cox MP. **2015**. HyLiTE: Accurate and flexible analysis of gene expression in hybrid and allopolyploid species. *BMC Bioinformatics* **16**: 1–4.

Duminil J, Hardy OJ, Petit RJ. **2009**. Plant traits correlated with generation time directly affect inbreeding depression and mating system and indirectly genetic structure. *BMC Evolutionary Biology* **9**: 1–14.

Edger PP, Smith R, McKain MR, Cooley AM, Vallejo-Marin M, Yuan Y, Bewick

AJ, Ji L, Platts AE, Bowman MJ, *et al.* 2017. Subgenome dominance in an interspecific hybrid, synthetic allopolyploid, and a 140-year-old naturally established neo-allopolyploid monkeyflower. *Plant Cell* **29**: 2150–2167.

Flagel LE, Wendel JF. **2010**. Evolutionary rate variation, genomic dominance and duplicate gene expression evolution during allotetraploid cotton speciation. *New Phytologist* **186**: 184–193.

Fyon F, Cailleau A, Lenormand T. **2015**. Enhancer Runaway and the Evolution of Diploid Gene Expression. *PLOS Genetics* **11**: e1005665.

Greer E, Martín AC, Pendle A, Colas I, Jones AME, Moore G, Shawa P. **2012**. The Ph1 Locus Suppresses Cdk2-Type Activity during Premeiosis and Meiosis in Wheat. *The Plant Cell* **24**: 152–162.

Griffiths AG, Moraga R, Tausen M, Gupta V, Bilton TP, Campbell MA, Ashby R, Nagy I, Khan A, Larking A, *et al.* 2019. Breaking free: The genomics of allopolyploidy-facilitated niche expansion in white clover. *Plant Cell* **31**: 1466–1487.

Grover CE, Gallagher JP, Szadkowski EP, Yoo MJ, Flagel LE, Wendel JF. **2012**. Homoeolog expression bias and expression level dominance in allopolyploids. *New Phytologist* **196**: 966–971.

Henry IM, Dilkes BP, Tyagi A, Gao J, Christensen B, Comaia L. **2014**. The BOY NAMED SUE Quantitative Trait Locus Confers Increased Meiotic Stability to an Adapted Natural Allopolyploid of *Arabidopsis*. *The Plant Cell* **26**: 181–194.

Hollister JD. **2015**. Polyploidy: adaptation to the genomic environment. *New Phytologist* **205**: 1034–1039.

Hollister JD, Gaut BS. **2009**. Epigenetic silencing of transposable elements: A trade-off between reduced transposition and deleterious effects on neighboring gene expression. *Genome Research* **19**: 1419–1428.

Hu G, Wendel JF. **2019**. *Cis – trans* controls and regulatory novelty accompanying allopolyploidization. *New Phytologist* **221**: 1691–1700.

Hurka H, Freundner S, Brown AHD, Plantholt U. **1989**. Aspartate aminotransferase isozymes in the genus *Capsella* (Brassicaceae): Subcellular location, gene duplication, and polymorphism. *Biochemical Genetics* **27**: 77–90.

Hurka H, Friesen N, German DA, Franzke A, Neuffer B. **2012**. 'Missing link' species *Capsella* orientalis and *Capsella thracica* elucidate evolution of model plant genus *Capsella* (Brassicaceae). *Molecular Ecology* **21**: 1223–1238.

Husband BC, Baldwin SJ, Sabara HA. **2016**. Direct vs. indirect effects of whole-genome duplication on prezygotic isolation in *Chamerion angustifolium*: Implications for rapid speciation. *American Journal of Botany* **103**: 1259–1271.

Jenczewski E, Eber F, Grimaud A, Huet S, Lucas MO, Monod H, Chèvre AM. **2003**. PrBn, a major gene controlling homeologous pairing in oilseed rape (*Brassica napus*) haploids. *Genetics* **164**: 645.

Johnson NA. **2010**. Hybrid incompatibility genes: remnants of a genomic battlefield? *Trends in Genetics* **26**: 317–325.

Katagiri Y, Hasegawa J, Fujikura U, Hoshino R, Matsunaga S, Tsukaya H. **2016**. The coordination of ploidy and cell size differs between cell layers in leaves.

Development (Cambridge) **143**: 1120–1125.

Kryvokhyzha D, Holm K, Chen J, Cornille A, Glémin S, Wright SI, Lagercrantz U, Lascoux M. **2016**. The influence of population structure on gene expression and flowering time variation in the ubiquitous weed *Capsella bursa-pastoris* (Brassicaceae). *Molecular Ecology* **25**: 1106–1121.

Kryvokhyzha D, Milesi P, Duan T, Orsucci M, Wright SI, Glémin S, Lascoux M. **2019a**. Towards the new normal: Transcriptomic convergence and genomic legacy of the two subgenomes of an allopolyploid weed (*Capsella bursa-pastoris*). *PLoS Genetics* **15**: e1008131.

Kryvokhyzha D, Salcedo A, Eriksson MC, Duan T, Tawari N, Chen J, Guerrina M, Kreiner JM, Kent T V., Lagercrantz U, *et al.* 2019b. Parental legacy, demography, and admixture influenced the evolution of the two subgenomes of the tetraploid *Capsella bursa-pastoris* (Brassicaceae). *PLoS Genetics* **15**: e1007949.

Lai D, Ha G, Shah S. **2022**. HMMcopy: Copy number prediction with correction for GC and mappability bias for HTS data. R package version 1.38.0.

Landis JB, Kurti A, Lawhorn AJ, Litt A, McCarthy EW. **2020**. Differential Gene Expression with an Emphasis on Floral Organ Size Differences in Natural and Synthetic Polyploids of *Nicotiana tabacum* (Solanaceae). *Genes 2020, Vol. 11, Page 1097* **11**: 1097.

Lashermes P, Combes MC, Hueber Y, Severac D, Dereeper A. **2014**. Genome rearrangements derived from homoeologous recombination following allopolyploidy speciation in coffee. *The Plant Journal* **78**: 674–685.

Lashermes P, Hueber Y, Combes M-C, Severac D, Dereeper A. **2016**. Inter-genomic DNA Exchanges and Homeologous Gene Silencing Shaped the Nascent Allopolyploid Coffee Genome (*Coffea arabica* L.).

Lesaffre T, Billiard S. **2020**. The joint evolution of lifespan and self-fertilization. *Journal of Evolutionary Biology* **33**: 41–56.

Levin DA. **1975**. MINORITY CYTOTYPE EXCLUSION IN LOCAL PLANT POPULATIONS. *TAXON* **24**: 35–43.

Li A, Liu D, Wu J, Zhao X, Hao M, Geng S, Yan J, Jiang X, Zhang L, Wu J, *et al.* 2014. mRNA and Small RNA Transcriptomes Reveal Insights into Dynamic Homoeolog Regulation of Allopolyploid Heterosis in Nascent Hexaploid Wheat. *The Plant Cell* **26**: 1878–1900.

Li M, Wang R, Wu X, Wang J. **2020**. Homoeolog expression bias and expression level dominance (ELD) in four tissues of natural allotetraploid *Brassica napus*. *BMC Genomics* **21**: 1–15.

Li N, Xu C, Zhang A, Lv R, Meng X, Lin X, Gong L, Wendel JF, Liu B. **2019**. DNA methylation repatterning accompanying hybridization, whole genome doubling and homoeolog exchange in nascent segmental rice allotetraploids. *New Phytologist* **223**: 979–992.

Lloyd A, Blary A, Charif D, Charpentier C, Tran J, Balzergue S, Delannoy E, Rigaill G, Jenczewski E. **2018**. Homoeologous exchanges cause extensive dosage-dependent gene expression changes in an allopolyploid crop. *New*

Phytologist **217**: 367–377.

Lunter G, Goodson M. **2011**. Stampy: A statistical algorithm for sensitive and fast mapping of Illumina sequence reads. *Genome Research* **21**: 936–939.

Lynch M, Conery JS. **2000**. The evolutionary fate and consequences of duplicate genes. *Science* **290**: 1151–1155.

Maherali H, Walden AE, Husband BC. **2009**. Genome duplication and the evolution of physiological responses to water stress. *New Phytologist* **184**: 721–731.

Martín AC, Rey MD, Shaw P, Moore G. **2017**. Dual effect of the wheat Ph1 locus on chromosome synapsis and crossover. *Chromosoma* **126**: 669–680.

Münzbergová Z. **2017**. Colchicine application significantly affects plant performance in the second generation of synthetic polyploids and its effects vary between populations. *Annals of Botany* **120**: 329–339.

Neuffer B, Paetsch M. **2013**. Flower morphology and pollen germination in the genus *Capsella* (Brassicaceae). *Flora - Morphology, Distribution, Functional Ecology of Plants* **208**: 626–640.

Nicolas SD, Leflon M, Monod H, Eber F, Coriton O, Huteau V, Chèvre AM, Jenczewski E. **2009**. Genetic Regulation of Meiotic Cross-Overs between Related Genomes in Brassica napus Haploids and Hybrids. *The Plant Cell* **21**: 373–385.

Novikova PY, Tsuchimatsu T, Simon S, Nizhynska V, Voronin V, Burns R, Fedorenko OM, Holm S, Säll T, Prat E, *et al.* 2017. Genome sequencing reveals the origin of the allotetraploid *Arabidopsis suecica*. *Molecular Biology and Evolution* **34**: 957–968.

Ohno S. **1970**. Evolution by Gene Duplication. *Evolution by Gene Duplication*.

Okonechnikov K, Conesa A, García-Alcalde F. **2016**. Qualimap 2: advanced multi-sample quality control for high-throughput sequencing data. *Bioinformatics* **32**: 292–294.

Paape T, Briskine R V., Halstead-Nussloch G, Lischer HEL, Shimizu-Inatsugi R, Hatakeyama M, Tanaka K, Nishiyama T, Sabirov R, Sese J, *et al.* 2018. Patterns of polymorphism and selection in the subgenomes of the allopolyploid *Arabidopsis kamchatica*. *Nature Communications* **9**: 3909.

Parisod C, Salmon A, Zerjal T, Tenaillon M, Grandbastien MA, Ainouche M. **2009**. Rapid structural and epigenetic reorganization near transposable elements in hybrid and allopolyploid genomes in Spartina. *New Phytologist* **184**: 1003–1015.

Pelé A, Rousseau-Gueutin M, Chèvre AM. **2018**. Speciation success of polyploid plants closely relates to the regulation of meiotic recombination. *Frontiers in Plant Science* **9**: 907.

R Core Team. **2020**. R: A language and environment for statistical computing. R Foundation for Statistical Computing.

Renny-Byfield S, Gong L, Gallagher JP, Wendel JF. **2015**. Persistence of Subgenomes in Paleopolyploid Cotton after 60 My of Evolution. *Molecular Biology and Evolution* **32**: 1063–1071.

Robinson MD, McCarthy DJ, Smyth GK. **2010**. edgeR: a Bioconductor package for differential expression analysis of digital gene expression data. *Bioinformatics* **26**: 139–140.

Roddy AB, Théroux-Rancourt G, Abbo T, Benedetti JW, Brodersen CR, Castro M, Castro S, Gilbride AB, Jensen B, Jiang GF, *et al.* 2020. The scaling of genome size and cell size limits maximum rates of photosynthesis with implications for ecological strategies. *International Journal of Plant Sciences* **181**: 75–87.

Roux C, Pannell JR. **2015**. Inferring the mode of origin of polyploid species from next-generation sequence data. *Molecular Ecology* **24**: 1047–1059.

Schindelin J, Arganda-Carreras I, Frise E, Kaynig V, Longair M, Pietzsch T, Preibisch S, Rueden C, Saalfeld S, Schmid B, *et al.* 2012. Fiji: An open-source platform for biological-image analysis. *Nature Methods* **9**: 676–682.

Schnable JC, Springer NM, Freeling M. **2011**. Differentiation of the maize subgenomes by genome dominance and both ancient and ongoing gene loss. *Proceedings of the National Academy of Sciences of the United States of America* **108**: 4069–4074.

Shan S, Boatwright JL, Liu X, Chanderbali AS, Fu C, Soltis PS, Soltis DE. **2020**. Transcriptome Dynamics of the Inflorescence in Reciprocally Formed Allopolyploid *Tragopogon miscellus* (Asteraceae). *Frontiers in Genetics* **11**: 888.

Shi X, Ng DWK, Zhang C, Comai L, Ye W, Jeffrey Chen Z. **2012**. Cis- and trans-regulatory divergence between progenitor species determines gene-expression novelty in *Arabidopsis* allopolyploids. *Nature Communications* **3**.

Slotte T, Hazzouri KM, Ågren JA, Koenig D, Maumus F, Guo YL, Steige K, Platts AE, Escobar JS, Newman LK, *et al.* 2013. The *Capsella rubella* genome and the genomic consequences of rapid mating system evolution. *Nature Genetics* **45**: 831–835.

Snodgrass SJ, Jareczek J, Wendel JF. **2017**. An examination of nucleotypic effects in diploid and polyploid cotton. *AoB Plants* **9**.

Sousa F, Neiva J, Martins N, Jacinto R, Anderson L, Raimondi PT, Serrão EA, Pearson GA. **2019**. Increased evolutionary rates and conserved transcriptional response following allopolyploidization in brown algae. *Evolution* **73**: 59–72.

Szadkowski E, Eber F, Huteau V, Lodé M, Huneau C, Belcram H, Coriton O, Manzanares-Dauleux MJ, Delourme R, King GJ, *et al.* 2010. The first meiosis of resynthesized *Brassica napus*, a genome blender. *New Phytologist* **186**: 102–112.

Tang H, Woodhouse MR, Cheng F, Schnable JC, Pedersen BS, Conant G, Wang X, Freeling M, Pires JC. **2012**. Altered Patterns of Fractionation and Exon Deletions in *Brassica rapa* Support a Two-Step Model of Paleohexaploidy. *Genetics* **190**: 1563.

Vicient CM, Casacuberta JM. **2017**. Impact of transposable elements on polyploid plant genomes. *Annals of Botany* **120**: 195–207.

Wang J, Tian L, Lee HS, Wei NE, Jiang H, Watson B, Madlung A, Osborn TC,

Doerge RW, Comai L, *et al.* 2006. Genomewide nonadditive gene regulation in *Arabidopsis* allotetraploids. *Genetics* **172**: 507–517.

Wang X, Zhang H, Li Y, Zhang Z, Li L, Liu B. **2016**. Transcriptome asymmetry in synthetic and natural allotetraploid wheats, revealed by RNA-sequencing. *New Phytologist* **209**: 1264–1277.

Wei Y, Li G, Zhang S, Zhang S, Zhang H, Sun R, Zhang R, Li F. **2021**. Analysis of Transcriptional Changes in Different *Brassica napus* Synthetic Allopolyploids. *Genes 2021, Vol. 12, Page 82* **12**: 82.

Wendel JF, Lisch D, Hu G, Mason AS. **2018**. The long and short of doubling down: polyploidy, epigenetics, and the temporal dynamics of genome fractionation. *Current Opinion in Genetics & Development* **49**: 1–7.

Wilson MJ, Fradera-Soler M, Summers R, Sturrock CJ, Fleming AJ. **2021**. Ploidy influences wheat mesophyll cell geometry, packing and leaf function. *Plant Direct* **5**: e00314.

Woodhouse MR, Cheng F, Pires JC, Lisch D, Freeling M, Wang X. **2014**. Origin, inheritance, and gene regulatory consequences of genome dominance in polyploids. *Proceedings of the National Academy of Sciences of the United States of America* **111**: 5283–5288.

Wu J, Lin L, Xu M, Chen P, Liu D, Sun Q, Ran L, Wang Y. **2018**. Homoeolog expression bias and expression level dominance in resynthesized allopolyploid *Brassica napus*. *BMC Genomics* **19**: 586.

Xiong Z, Gaeta RT, Edger PP, Cao Y, Zhao K, Zhang S, Chris Pires J. **2021**. Chromosome inheritance and meiotic stability in allopolyploid *Brassica napus*. *G3 Genes|Genomes|Genetics* **11**.

Ye B, Wang R, Wang J. **2016**. Correlation analysis of the mRNA and miRNA expression profiles in the nascent synthetic allotetraploid *Raphanobrassica*. *Scientific Reports 2016 6:1* **6**: 1–15.

Yoo MJ, Szadkowski E, Wendel JF. **2013**. Homoeolog expression bias and expression level dominance in allopolyploid cotton. *Heredity* **110**: 171–180.

Yu X, Zhai Y, Wang P, Cheng C, Li J, Lou Q, Chen J. **2021**. Morphological, anatomical and photosynthetic consequences of artificial allopolyploidization in Cucumis. *Euphytica* **217**: 1–13.

Zhang D. **2022**. rsq: R-Squared and Related Measures. R package version 2.5.

Zhang H, Bian Y, Gou X, Zhu B, Xu C, Qi B, Li N, Rustgi S, Zhou H, Han F, *et al.* 2013. Persistent whole-chromosome aneuploidy is generally associated with nascent allohexaploid wheat. *Proceedings of the National Academy of Sciences of the United States of America* **110**: 3447–3452.

Zhang H, Gou X, Zhang A, Wang X, Zhao N, Dong Y, Li L, Liu B. **2016a**. Transcriptome shock invokes disruption of parental expression-conserved genes in tetraploid wheat. *Scientific Reports 2016 6:1* **6**: 1–11.

Zhang D, Pan Q, Tan C, Zhu B, Ge X, Shao Y, Li Z. **2016b**. Genome-Wide Gene Expressions Respond Differently to A-subgenome Origins in Brassica napus Synthetic Hybrids and Natural Allotetraploid. *Frontiers in plant science* **7**.

Figures and Tables

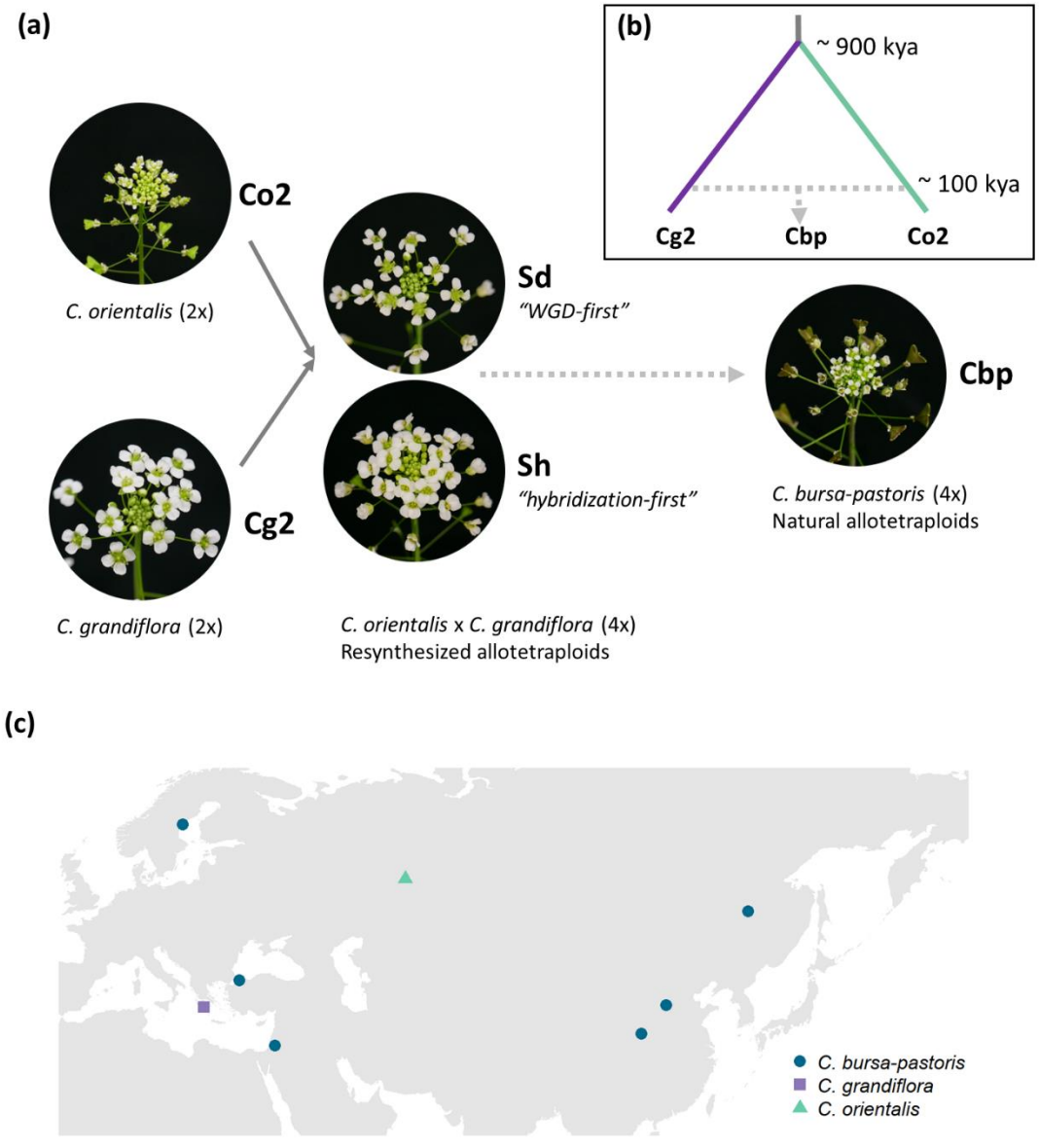

Fig. 1 Plant material used in the present study. (a) Five groups of *Capsella* plants. Diploid species (Co2 and Cg2 groups) and the second generation of resynthesized allotetraploids (Sd and Sh groups) were from Duan *et al.* (2023). Samples of natural allotetraploids, *C. bursa-pastoris*, were added to the present study. (b) Phylogenetic relationship of the three natural species used in the present study, modified from Douglas *et al.*, (2015); *C. bursa-pastoris* originated from the hybridization between the ancestral population of *C. orientalis* and the (*C. grandiflora* + *C. rubella*) lineage, and *C. rubella* were omitted from the figure; kya: thousand years ago. (c) Geographic origin of the *Capsella* samples.

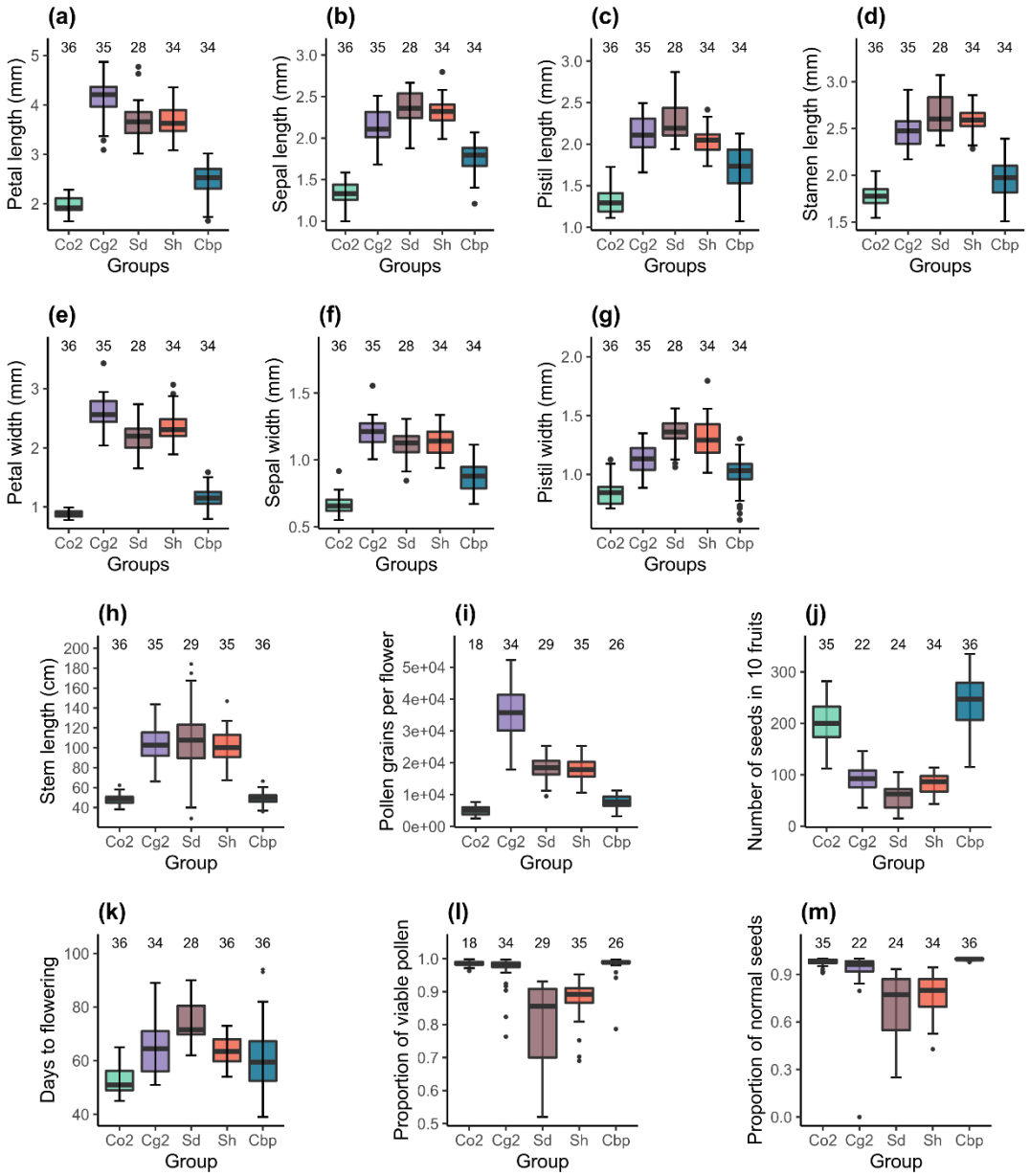

Fig. 2 Phenotypic traits of the five *Capsella* groups. Co2: diploid *C. orientalis*; Cg2: diploid *C. grandiflora*; Sd: WGD-first resynthesized allotetraploids; Sh: hybridization-first resynthesized allotetraploids; Cbp: natural allotetraploid *C. bursa-pastoris*. The measured traits were (a) petal length, (b) sepal length, (c) pistil length, (d) stamen length, (e) petal width, (f) sepal length, (g) pistil width, (h) length of the longest stem, (i) number of pollen grains per flower, (j) number of seeds in ten fruits, (k) number of days from germination to the opening of the first flower, (l) proportion of viable pollen grains, and (m) proportion of normal seeds in ten fruits.

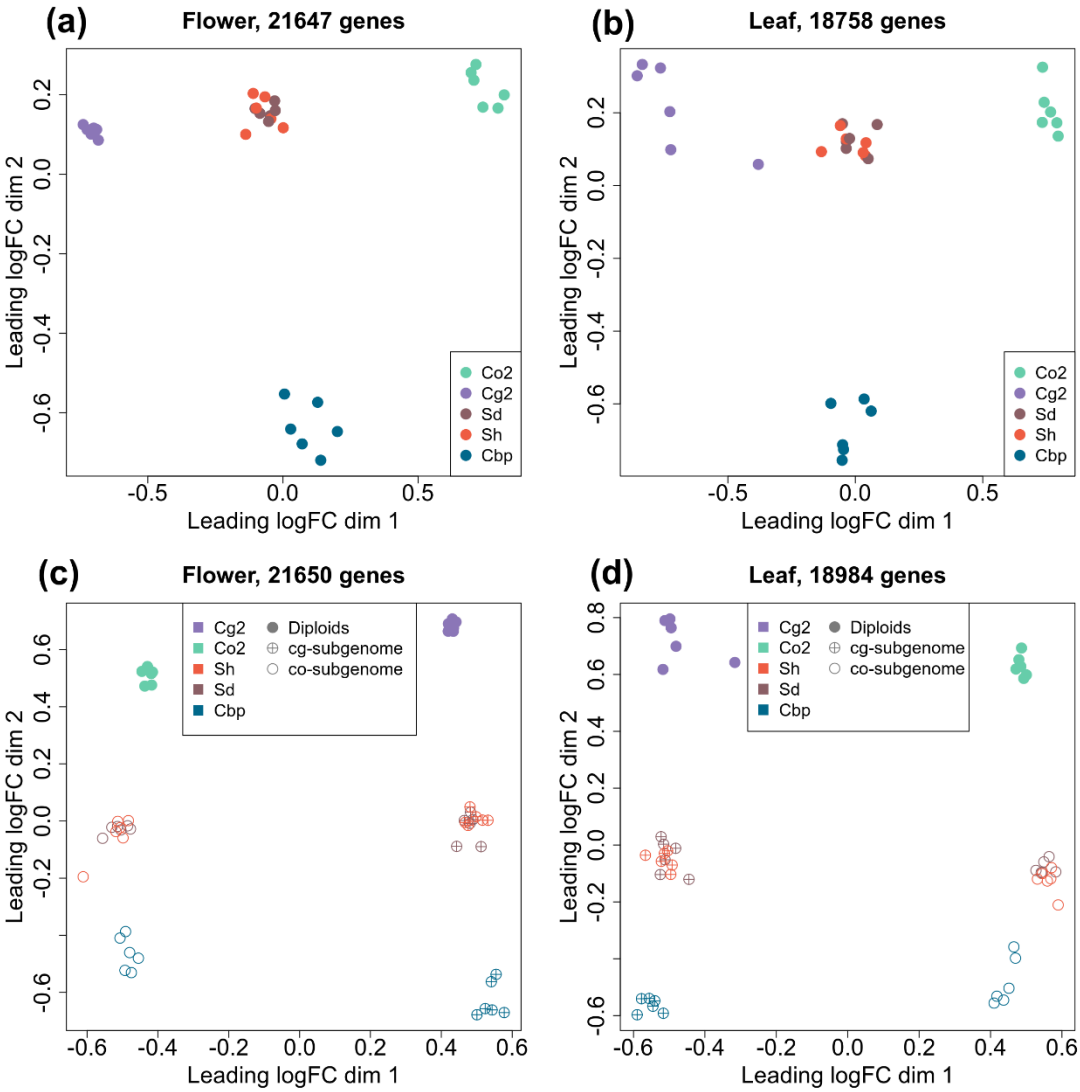

Fig. 3 Multi-dimensional scaling (MDS) analyses of gene or homoeolog expression in two tissues. Down-sampled gene expressions were used to compare gene expression patterns of the five plant groups in either flowers (a) or leaves (b). Separated homoeolog expressions in allotetraploids were then compared with rescaled gene expression of diploid groups in both flowers (c) and leaves (d). All the MDS analyses used genes with count-per-million (CPM) > 1 in at least two samples, and expression levels were normalized with the trimmed mean of M-values (TMM) method.

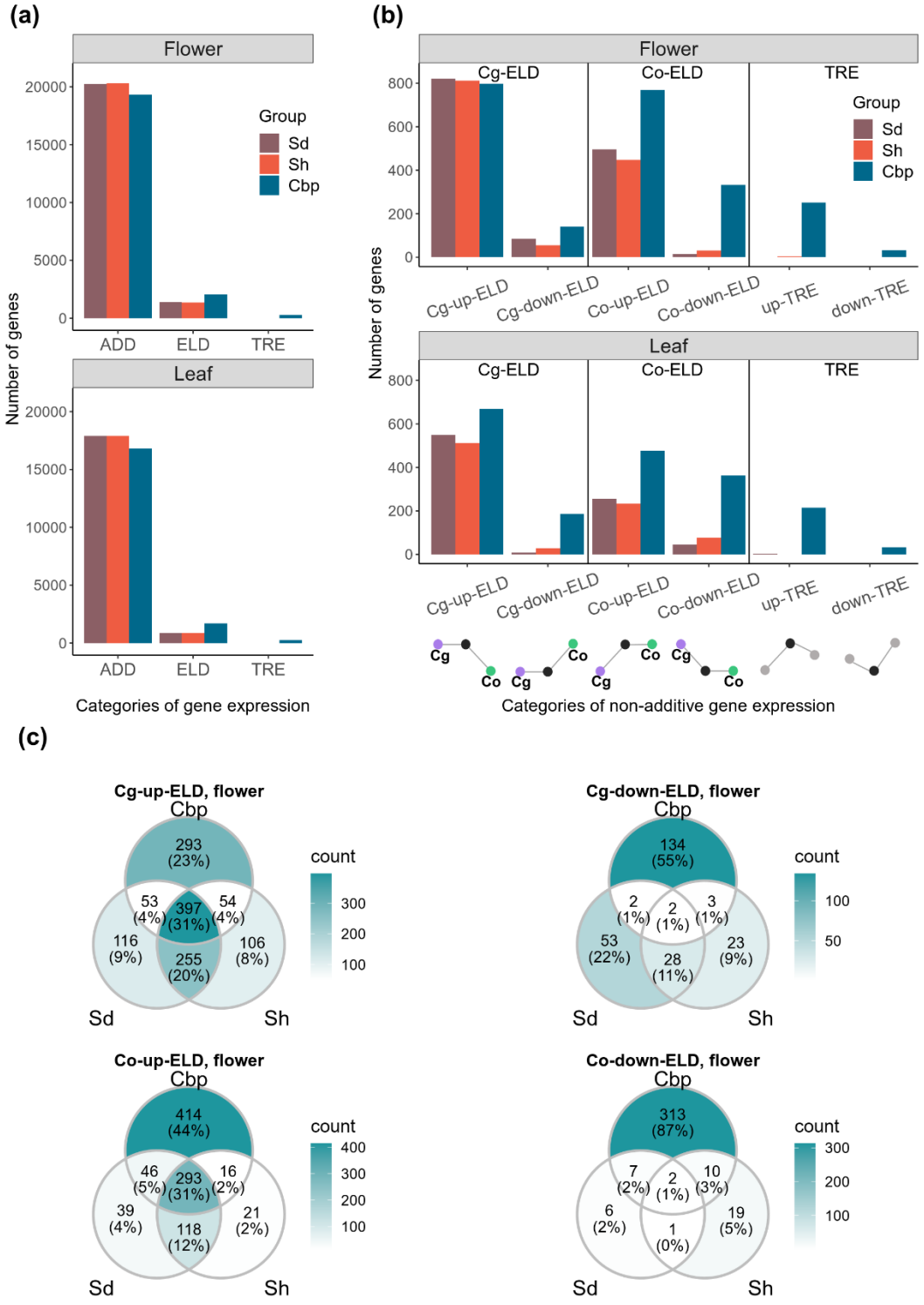

Fig. 4 Additive and non-additive expression in allotetraploid groups. a) Number of genes that showed additive expression (ADD, including partial expression level dominance), complete expression level dominance (ELD), and transgressive expression (TRE) in each allotetraploid group. b) Genes with complete ELD or TRE were further classified by whether they were up- or down-regulated in allotetraploids, and whether the expression level in allotetraploids was similar to *C. grandiflora* (Cg-ELD) or *C. orientalis* (Co-ELD). c) Venn diagram of genes with complete ELD of the three allotetraploid groups in flowers, separated by directions of ELD.

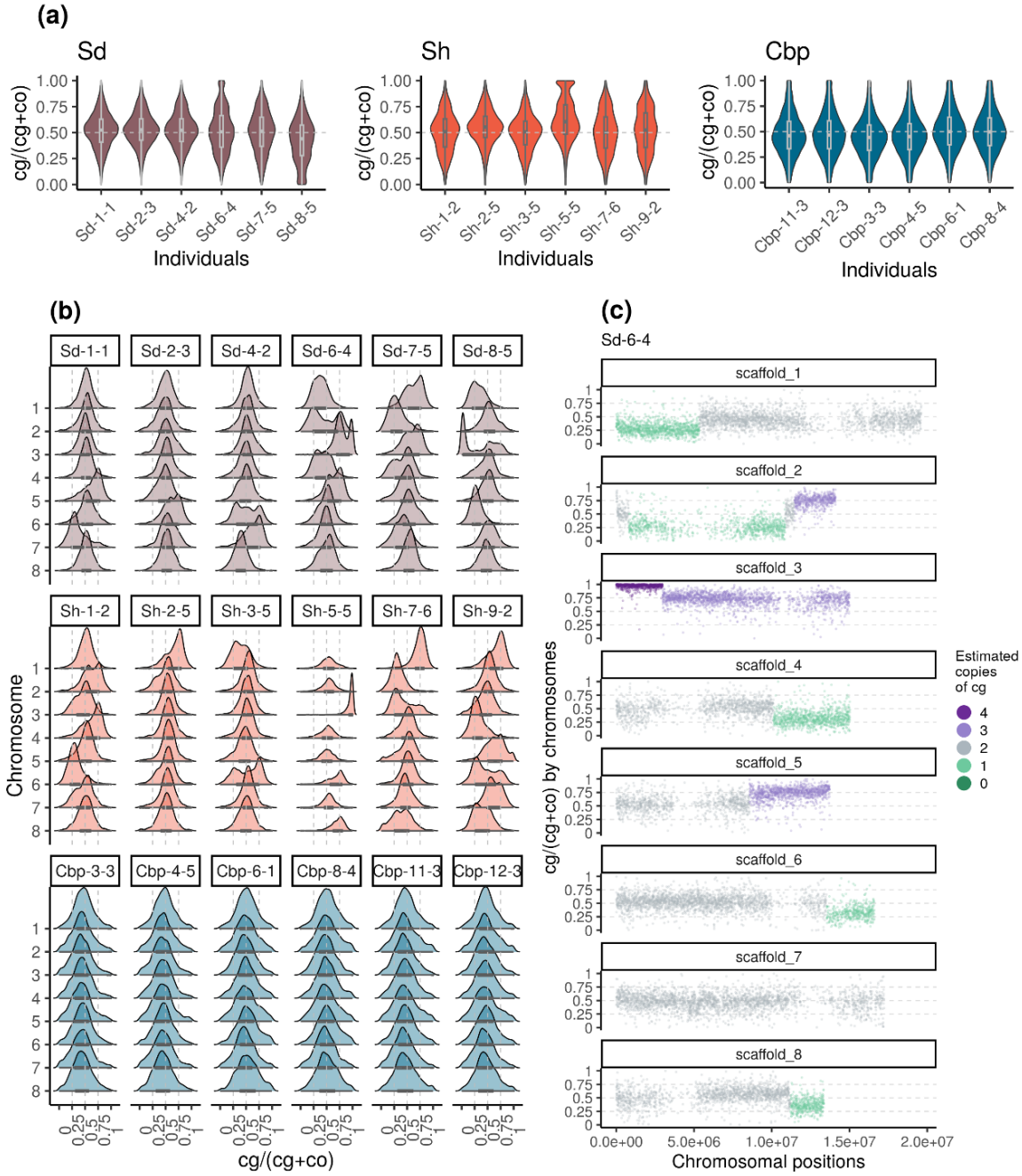

Fig. 5 Variation of homoeolog expression bias (HEB) of the three allotetraploid groups in flowers. Gene HEB was calculated as the expression level of cg-homoeolog divided by the total expression level of both cg- and co- homoeologs (HEB = cg/(cg+co)). For each individual, HEB was calculated for 18,255 genes, which had count-per-million > 1 in all flower samples. The distribution of gene HEB was shown by (a) individuals and (b) chromosomes. (c) Gene HEB was also plotted along chromosome positions to show the sudden change of mean HEB between genomic blocks, taking individual Sd-6-4 as an example. The number of cg-homoeologs at each gene estimated by the five-state Hidden Markov Model (HMM) was indicated by five colors. Dark green, light green, grey, light purple and dark purple represent (0, 1, 2, 3, 4) cg-homoeologs and (4, 3, 2, 1, 0) co-homoeologs, respectively.

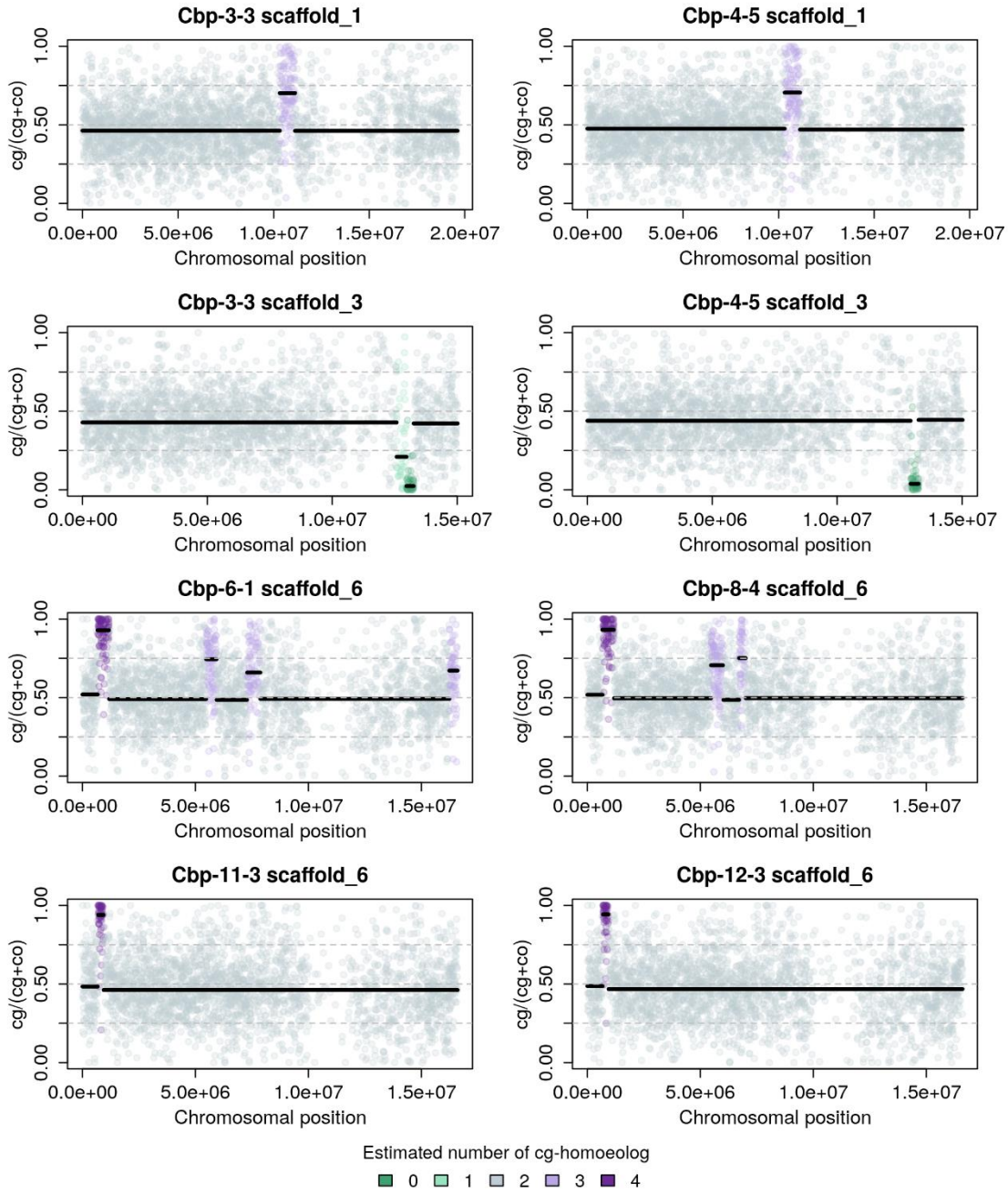

Fig. 6 Homoeolog expression bias (cg/(cg+co)) along chromosomes of natural *C. bursa-pastoris* in flowers, taking four pairs of chromosome quartets with typical patterns as an example. The number of cg-homoeologs estimated by the five-state Hidden Markov Model was indicated by five colors. The two chromosome quartets in the same row are from the two individuals of the same major genetic cluster of natural *C. bursa-pastoris* (Kryvokhyzha *et al.*, 2016, 2019b), showing that some estimated segments with an unbalanced number of cg- and co-homoeologs were shared between the individuals from the same genetic cluster.

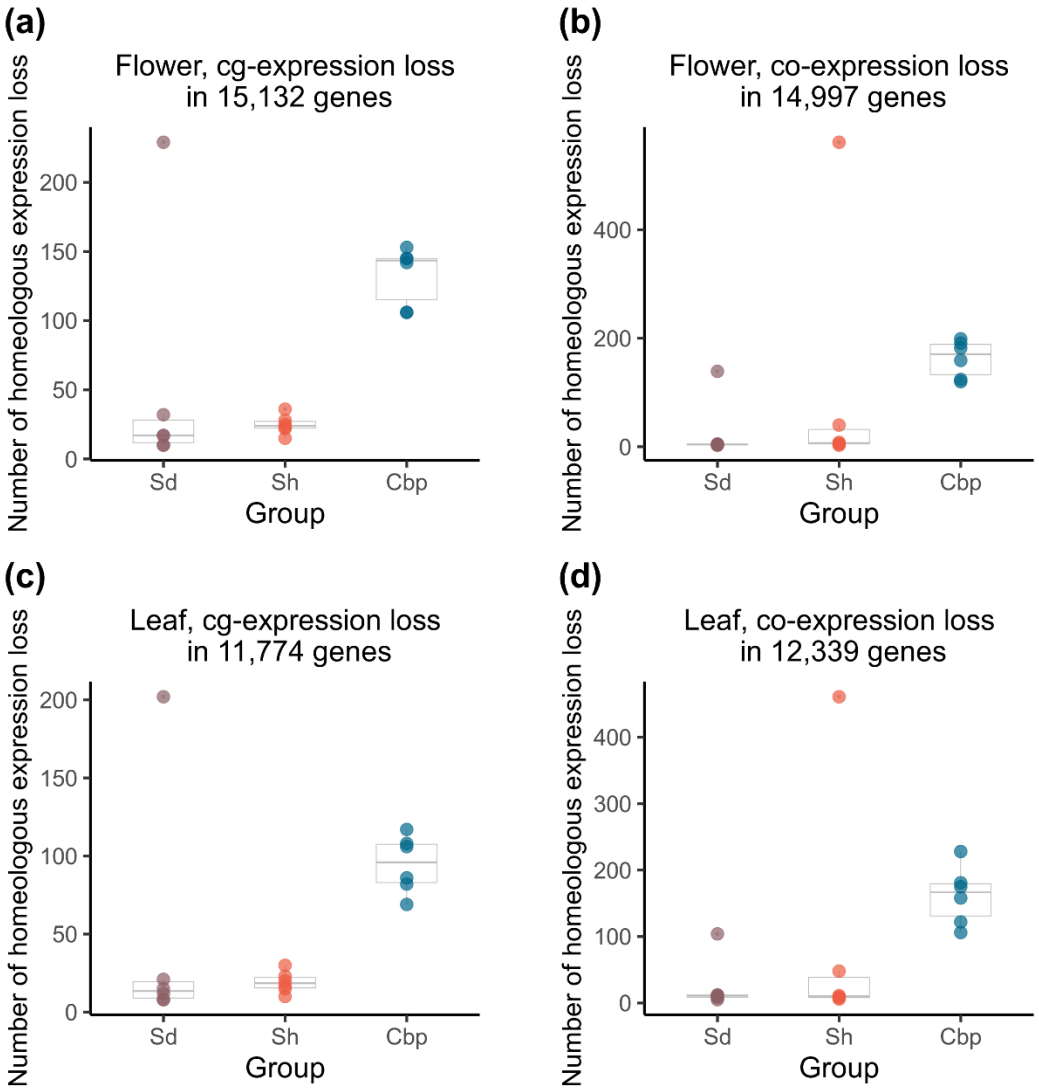

Fig. 7 Loss of homoeolog expression in resynthesized (Sd and Sh) and natural allotetraploids (Cbp). The number of genes with homoeolog expression loss per individual was compared among the three groups of allotetraploids in flowers (a,b) or leaves (c,d). Homoeologous genes that had obvious expression (count per million > 5) in all individuals of the corresponding diploid species but almost no expression (count per million < 0.5) in one allotetraploid individual were considered cases of homoeolog expression loss.

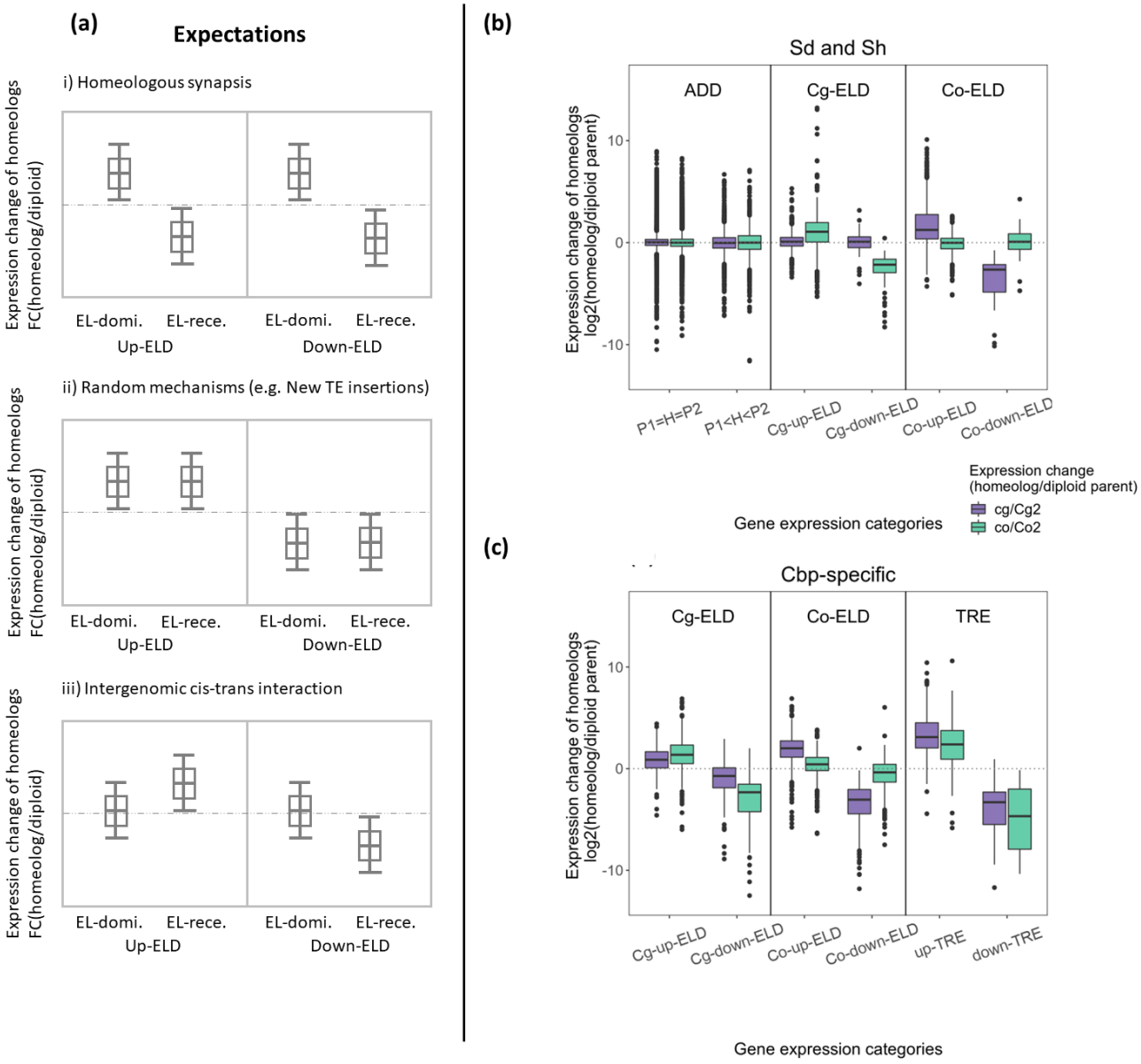

Fig. 8 Relationships between homoeolog expression change and non-additive gene expression in flowers. (a) Expected patterns of homoeolog expression change in each scenario that may explain the cause of ELD in resynthesized allotetraploids. (b) Observed homoeolog expression change among genes with ELD in resynthesized allotetraploids. (c) Observed homoeolog expression change among genes with Cbp-specific non-additive expression.

Table 1 Classification of additive and non-additive gene expression pattern in allotetraploids

Group	Description	Classification criteria
a	Additive expression with no parental differentiation	$Cg_i = x_{ij} = Co_i$
b	Partial ELD or additive expression with parental differentiation	$(Cg_i < x_{ij} < Co_i)$ or $(Co_i < x_{ij} < Cg_i)$ or $(Cg_i \neq Co_i$ and $x_{ij} = Cg_i$ and $x_{ij} = Co_i)$
c	Up-regulated ELD toward Cg2	$x_{ij} = Cg_i$ and $x_{ij} > Co_i$
d	Down-regulated ELD toward Cg2	$x_{ij} = Cg_i$ and $x_{ij} < Co_i$
e	Up-regulated ELD toward Co2	$x_{ij} = Co_i$ and $x_{ij} > Cg_i$
f	Down-regulated ELD toward Co2	$x_{ij} = Co_i$ and $x_{ij} < Cg_i$
g	Up-regulated TRE with no parental differentiation	$Cg_i = Co_i$ and $x_{ij} > Cg_i$ and $x_{ij} > Co_i$
h	Up-regulated TRE with parental differentiation	$Cg_i \neq Co_i$ and $x_{ij} > Cg_i$ and $x_{ij} > Co_i$
i	Down-regulated TRE with no parental differentiation	$Cg_i = Co_i$ and $x_{ij} < Cg_i$ and $x_{ij} < Co_i$
j	Down-regulated TRE with parental differentiation	$Cg_i \neq Co_i$ and $x_{ij} < Cg_i$ and $x_{ij} < Co_i$

* Cg_i: expression level of gene i in the Cg2 group; Co_i: expression level of gene i in the Co2 group; x_{ij}: expression level of gene i in allotetraploid group j, and $j \in$ (Sd, Sh, Cbp); ELD: expression level dominance; TRE: transgressive expression; The significance of differential expression between groups were determined by results of differential expression analysis on unphased gene expression, with a threshold of fold-change > 2 and false discovery rate < 0.05.